RESEARCH ARTICLE | APRIL 15 2010

Lysophosphatidylcholine Increases Neutrophil Bactericidal Activity by Enhancement of Azurophil Granule-Phagosome Fusion via Glycine·GlyRα2/TRPM2/p38 MAPK Signaling `FREE`

Chang-Won Hong; ... et. al

Related Content

Correction: Lysophosphatidylcholine Increases Neutrophil Bactericidal Activity by Enhancement of Azurophil Granule-Phagosome Fusion via Glycine·GlyRα2/TRPM2/p38 MAPK Signaling

J Immunol (August,2010)

IN THIS ISSUE

J Immunol (April,2010)

The impact of the TRPM2 ion channel on inflammation and macrophage metabolism in gastrointestinal models

J Immunol (May,2019)

Lysophosphatidylcholine Increases Neutrophil Bactericidal Activity by Enhancement of Azurophil Granule-Phagosome Fusion via Glycine·GlyRα2/TRPM2/p38 MAPK Signaling

Chang-Won Hong,*[,1] Taek-Keun Kim,*[,1] Hwa-Yong Ham,* Ju-Suk Nam,*
Yong Ho Kim,[†] Haifeng Zheng,[‡] Bo Pang,[‡] Tae-Kwon Min,* Jun-Sub Jung,*
Si-Nae Lee,* Hyun-Jeong Cho,* Ee-Jin Kim,* In-Hwan Hong,* Tae-Cheon Kang,[§]
Jongho Lee,* Seog Bae Oh,[†] Sung Jun Jung,[¶] Sung Joon Kim,[‡] and Dong-Keun Song*

Neutrophils are the first-line defense against microbes. Enhancing the microbicidal activity of neutrophils could complement direct antimicrobial therapy for controlling intractable microbial infections. Previously, we reported that lysophosphatidylcholine (LPC), an endogenous lipid, enhances neutrophil bactericidal activity (Yan et al. 2004. *Nat. Med*. 10: 161–167). In this study we show that LPC enhancement of neutrophil bactericidal activity is dependent on glycine, and is mediated by translocation of intracellularly located glycine receptor (GlyR) α2 to the plasma membrane, and subsequent increase in azurophil granule-phagosome fusion/ elastase release. LPC induced GlyRα2-mediated $[Cl^-]_i$ increase, leading to transient receptor potential melastatin (TRPM)2-mediated Ca^{2+} influx. Studies using human embryonic kidney 293 cells heterologously expressing TRPM2 and neutrophils showed that TRPM2 channel activity is sensitive to $[Cl^-]_i$. Finally, LPC induced p38 MAPK phosphorylation in an extracellular calcium/ glycine dependent manner. SB203580, a p38 MAPK inhibitor, blocked LPC-induced enhancement in Lucifer yellow uptake, azurophil granule-phagosome fusion, and bactericidal activity. These results propose that enhancement of azurophil granule- phagosome fusion via GlyRα2/TRPM2/p38 MAPK signaling is a novel target for enhancement of neutrophil bactericidal activity. *The Journal of Immunology*, 2010, 184: 4401–4413.

The recent increasing emergence of antibiotic-resistant microorganisms and the current paucity of novel antibiotics present a serious threat to human health (1, 2). Neutrophils are the first-line defense against microbial infections (for review, see Ref. 3). Compared with conventional antimicrobial therapy, enhancement of neutrophil microbicidal activity, in theory, has the advantage of effectiveness against a broad spectrum of even antimicrobial-resistant microbes. This approach could

therefore be a successful strategy, complementing standard antimicrobial agents, for controlling serious microbial infections (4).

Lysophosphatidylcholine (LPC) is an endogenous immunomodulatory lipid, with its plasma concentration being ~200 μM (for review, see Ref. 5). LPC has various stimulating or modulating activities on neutrophils (6–9). Previously we reported that systemic administration of LPC to mice enhances bacterial clearance in vivo (10). LPC does not have direct antibacterial activity, but enhances the bactericidal activity of neutrophils (10). Many reports showed that LPC enhances reactive oxygen species production by neutrophils (6, 9–13). The precise mechanisms of LPC enhancement of neutrophil bactericidal activity, however, remain largely unknown.

NADPH oxidase and the resultant reactive oxygen species play a pivotal role in neutrophil bactericidal activity (for review, see Ref. 14). More recently, an important, direct role for neutophil proteases (such as neutrophil elastase and cathepsin G) in microbicidal activity was revealed (15–18). Cooperation between neutrophil antimicrobial weapons also exists (for review, see Ref. 19). In addition, neutrophil extracellular traps were found to be important for extracellular bactericidal activity (20). In light of these various mechanisms of neutrophil bactericidal activity, we focused in this study on investigating the mechanism of LPC-induced enhancement of neutrophil bactericidal activity.

In this study, we present evidence that LPC enhancement of neutrophil bactericidal activity depends on glycine, and is mediated by translocation of glycine receptor (GlyR) α2 to the plasma membrane and subsequent induction of fluid-phase pinocytosis and the enhanced fusion of phagosome with azurophil granules, with the accompanying enhanced release of elastase, for which GlyRα2/transient receptor potential melastatin (TRPM)2/p38 MAPK signaling plays an essential role.

*Department of Pharmacology, Institute of Natural Medicine, Infectious Diseases Medical Research Center and [§]Department of Anatomy and Neurobiology, College of Medicine, Hallym University, Chuncheon; [†]Department of Physiology, School of Dentistry and [‡]Department of Physiology, College of Medicine, Seoul National University; and [¶]Department of Physiology, Hanyang University School of Medicine, Seoul, Korea

[1]C-W.H. and T-K.K. contributed equally to this work.

Address correspondence and reprint requests to Dr. Dong-Keun Song or Dr. Sung Joon Kim, Department of Pharmacology, Institute of Natural Medicine, Infectious Diseases Medical Research Center, Hallym University College of Medicine, 39 Hallymdaehak-gil, Chuncheon, Gangwon-do 200-702, South Korea (D.-K.S.) or Department of Physiology, College of Medicine, Seoul National University, 103 Daehangno, Jongno-gu, Seoul 110-799, South Korea (S.J.K.). E-mail addresses: dksong@hallym.ac.kr or sjoonkim@snu.ac.kr

The online version of this article contains supplemental material.

Abbreviations used in this paper: ADPR, adenosine 5′-diphosphoribose; CLP, cecal ligation and puncture; DPI, diphenylene iodonium; F/Fo, fluorescence intensity ratio; GlyR, glycine receptor; HEK, human embryonic kidney; HEPES-PSS, HEPES physiologic salt solution; LPC, lysophosphatidylcholine; MQAE, *N*-(6-methoxyquinolyl) acetoethyl ester; PTX, pertussis toxin; ProI, protease inhibitor mixture; TRP, transient receptor potential; TRPM, transient receptor potential melastatin.

Materials and Methods

Reagents used

LPC (18:0) was obtained from Sigma-Aldrich Chemical (St. Louis, MO), and 3 mM stock solution in PBS was prepared with sonication. Strychnine, valinomycin, pertussis toxin (PTX), Lucifer yellow, econazole, clotrimazole, flufenamic acid, and adenosine 5′-diphosphoribose (ADPR) were from Sigma-Aldrich. Diphenylene iodonium (DPI) and SB203580 were from Tocris Bioscience (Ellisville, MO). CytofixTM, FITC anti-CD63 Ab, Alexa Fluor 488 anti–phosphor-p38 Ab, Phosflow Buffer I, and Phosflow Perm Buffer II were from BD Pharmingen (San Diego, CA). Enz Chek Elastase assay kit, Texas red-labeled zymosan particles, Fluo-3 AM, and N-(6-methoxyquinolyl) acetoethyl ester (MQAE) were from Molecular Probes (San Diego, CA). Alexa Fluor 594 rabbit anti-goat IgG F(ab′)2 and Alexa Fluor 488 anti-mouse secondary Ab were from Invitrogen (San Diego, CA). Anti-GlyRα2 Ab (N-18) and anti-actin Ab were from Santa Cruz Biotechnology (Santa Cruz, CA). shRNAmir targeting GlyRα2 and TRPM2 were from Open Biosystems (Huntsville, AL).

Preparation of neutrophils

Neutrophils were purified from heparinized venous blood from healthy volunteer donors. In brief, neutrophils were isolated by density centrifugation in Histopaque-1077, followed by dextran sedimentation. Residual erythrocytes were eliminated with hypotonic lysis. The purity of neutrophils counted by Diff Quik staining was >95% on average. The viability of neutrophils stained with tryphan blue was >99%. After isolation procedure, neutrophils were dispersed in RPMI 1640 supplemented with 5% FBS.

Assay of bactericidal activity of human neutrophils

Bactericidal activity of human neutrophils was measured as slightly modified from the method described previously (10, 21). In brief, neutrophils (4×10^6/ml, 0.5 ml) were seeded on a 13-mm plastic coverslip (coated overnight with 0.05% poly-L-lysine) in 24-well plate for 1 h in a humidified CO_2 incubator (5% CO_2 and 95% air atmosphere). Coverslips were then transferred to 60-mm dish (6 coverslips/dish) containing 2×10^7 Escherichia coli (overnight cultured E. coli [DH5-α] were opsonized with 10% human serum for 30 min) at a neutrophil/E. coli ratio of 1:10 for 20 min for E. coli uptake. After the 20 min uptake, 18.3 ± 1.9% (mean ± SEM, n = 2) of E. coli was removed by adherent neutrophils. Coverslips were then transferred to 24-well plate containing 500 μl RPMI 1640 (supplemented with 5% FBS) containing vehicle or LPC (30 μM). After 15 min, coverslips were transferred to 24-well plate with ice-cold distilled water for 1 h for lysis of neutrophils (CFUs after 15 min incubation). For evaluation of total number of phagocytosed E. coli, some coverslips were directly transferred to ice-cold distilled water after 20 min of E. coli uptake without an additional 15-min incubation with LPC (CFUs before 15 min incubation). E. coli were plated in Lysogeny broth agar plate and cultured overnight at 37°C and viable colony was counted. The percentage of bacteria killed was calculated as 100 × (1 – CFUs after 15 min incubation/CFUs before 15 min incubation). For effects of various inhibitors, assay of bactericidal activity was performed in the presence of strychnine (1 μM), DPI (1 μM), protease inhibitor mixture (leupeptin 10 μg/ml, N-tosyl-L-leucin chloromethyl ketone 10 μg/ml, pepstatin A 10 μg/ml, aprotinin 10 μg/ml, and PMSF 1 mM), or SB203580 (10 μM). To evaluate the effect of glycine on LPC-induced enhancement of bactericidal activity, glycine-supplemented HBSS was used. For chloride-free media, chloride in HBSS was replaced with equimolar gluconate (mM) (glucose 15.13, magnesium sulfate 8.14, dibasic sodium phosphate 0.34, monobasic potassium phosphate 0.44, calcium gluconate 1.26, potassium gluconate 5.4, sodium gluconate 136.8). All media was supplemented with 5% FBS. In a subset of experiment (Supplemental Fig. 1), a different assay method for neutrophil bactericidal activity was used (22, 23). In brief, neutrophils (4×10^6/ml) in RPMI 1640 with 10% human serum were incubated with opsonized E. coli (4×10^7/ml) for 3 min with continuous rotation to promote phagocytosis. After removal of noningested bacteria with differential centrifugation at 110g for 4 min, neutrophils resuspended were incubated at 37°C for 10 min with slow rotation in the presence of LPC. Killing was stopped by spinning the neutrophils at 110g for 5 min onto ice after addition of distilled water (pH 11). The 10-fold diluted E. coli were plated in Lysogeny broth agar plate and cultured overnight at 37°C and the viable colony was counted. The percentage of bacteria killed was calculated as 100 × (1 – CFUs after 10 min incubation/CFUs before 10 min incubation).

Assay of elastase release

Neutrophils (2×10^6/well) in RPMI 1640 (supplemented with 5% FBS) were incubated in 96-well plate for 1 h. Then, opsonized E. coli (2×10^6/well) and

LPC (30 μM) or vehicle were added. After an additional 1-h incubation, elastase release was measured in the supernatants with Enz Chek Elastase assay kit. Some experiments were performed with strychnine (1 μM) throughout the 2 h.

Flow cytometry

For the analysis of surface expression of CD63, neutrophils were stimulated with LPC 30 μM for 5 min in RPMI 1640 (supplemented with 5% FBS). Cells were fixed with CytofixTM for 5 min. After washing, neutrophils were stained with FITC conjugated anti-CD63 Ab for 30 min on ice. Neutrophils were acquired on Guava Easycyte (GE Healthcare, Buckinghamshire, U.K.) and analysis was performed using FCS express V3 (De Novo Software, Los Angeles, CA). The expression of phospho-p38 in neutrophils was measured by FACS using BDTM Phosflow technique. Neutrophils were stimulated with LPC 30 μM for 5 min in RPMI 1640 (supplemented with 5% FBS). Cells were fixed in Phosflow Buffer I for 15 min. After washing, permeabilization was done with Phosflow Perm Buffer II for 30 min on ice. Then, neutrophils were washed and stained with Alexa 488 anti–phosphor-p38 Ab for 30 min at room temperature.

Fusion of azurophil granule and zymosan

Texas red-labeled zymosan particles were incubated in 10% human serum for 20 min at 37°C, washed twice with PBS, pH 7.4, and resuspended in PBS. Neutrophils (4×10^6/ml) were plated on glass coverslips and incubated at 37°C for 1 h in 24-well culture plate. Coverslips were then transferred to 60-mm dish containing Texas red-labeled zymosan at a ratio of 1:10. After 20 min, neutrophils were washed to remove most of the extracellular Texas red-labeled zymosan. Neutrophils were transferred to 24-well plate and LPC 30 μM was added. After 15 min, zymosan-loaded neutrophils were washed twice with PBS and fixed using 2% paraformaldehyde for 15 min at room temperature, followed by permeabilization using 0.05% Triton X-100 for 10 min at room temperature. After 1-h blocking period in PBS containing 3% BSA, the neutrophils were incubated for 1 h with an anti-CD63 Ab (1:50 in blocking buffer). After 1 h incubation at room temperature, cells were washed three times in PBS and were incubated for 1 h with the Alexa Fluor 488 anti-mouse secondary Ab (1:500). After three washes in PBS, the cells were mounted using mounting medium. Azurophil granule-phagosome fusion was calculated by measuring colocalized area between CD63 (an azurophil granule marker) and zymosan particles, which was divided by intracellular total zymosan area in confocal images of neutrophils. Stacks of 12–16 confocal images were collected with a LSM 510 laser-scanning confocal microscope (Carl Zeiss, Jena, Germany). Image analysis was performed using LSM Image Examiner software (Carl Zeiss). The images illustrate a single section with 0.52-μM thickness.

Cecal ligation and puncture

Cecal ligation and puncture (CLP) was performed as described previously (10). Male ICR mice at the age of 6 wk (25–28 g body weight) were used. Procedures for animal experiments were approved by the Animal Experimentation Committee at Hallym University. Mice were anesthetized with pentobarbital (50 mg/kg, i.p.), and a small abdominal midline incision was made and the cecum was exposed. The cecum was mobilized and ligated below the ileocecal valve, punctured through both surfaces two times with a 22-gauge needle, and the abdomen was closed. Mice were pretreated with PBS or strychnine (0.4 mg/kg, s.c.) 30 min before each injection of vehicle (PBS containing 2% BSA) or LPC (10 mg/kg, s.c.) (four times at 12 h intervals beginning 2 h after CLP). Survival was monitored once daily for 10 d. For determination of bacterial clearance in vivo, mice were pretreated with PBS or strychnine (0.3 mg/kg, s.c.) 30 min prior to each injection of vehicle (PBS containing 2% BSA) or LPC (10 mg/kg, s.c.) at 2 h and 11 h after CLP. Eighteen hours after CLP, mice were anesthetized and peritoneal lavage fluid was collected and cultured overnight on Trypticase Soy Agar (BD Biosciences, San Jose, CA) at 37°C and the numbers of CFUs were counted.

Measurement of Lucifer yellow uptake

Lucifer yellow uptake into neutrophils was measured as described previously (24). Neutrophils (4×10^6/ml) were incubated with 0.5 mg/ml Lucifer yellow 37°C for 15, 30 and 60 min in RPMI 1640 (supplemented with 5% FBS) in the presence of LPC 30 μM or vehicle (PBS). Then, neutrophils were washed two times with cold PBS and lysed with ice-cold deionized distilled water for 1 h. The Lucifer yellow uptake was measured with Spectramax M2/e fluorescence microplate reader (Molecular Devices, Sunnyvale, CA) at 428 nm excitation and 536 nm emission. In some experiments, neutrophils were incubated with E. coli at a ratio of 1:10 for 20 min. After washing unengulfed E. coli, neutrophils were

further incubated with LPC or vehicle for 15 min in the presence of Lucifer yellow. All media were supplemented with 5% FBS.

RT-PCR

Total RNA was isolated from human neutrophils using TRIzol reagent (Invitrogen) according to the manufacturer's protocol. The first strand cDNA was synthesized with SuperScriptII (Invitrogen), and one tenth of the cDNA was used for each PCR. The sequences of the PCR primers are as follows: GlyRα1, 5′-TGCAATAGCGCTTTCTGGTT-3′ (forward) and 5′-TCCGGGAGATCCTTAGCAAT-3′ (reverse); GlyRα2, 5′-GCCAAA-TTTTAAAGGTCCTCCAIIIIICGTTACTTGC-3′ (forward) (Seegene) and 5′-GTCAGTGGTGACATCGTGGAAGIIIIIACCCTTCTCA-3′ (reverse) (Seegene); GlyRα3, 5′-TTCCTCCAATCCTGG GTCTC-3′ (forward) and 5′-TCCTGATGTCCTGCCCATTA-3′ (reverse); GlyRβ, 5′-TGGACTT-GACACTGTTTCCCAIIIIIACACAACG-3′ (forward) (Seegene) and 5′-TCAGATCAGACTTGGAAGTACAAACTIIIIIGCATCTGG-3′ (reverse) (Seegene); β-actin, 5′-TGGAGTCCTGTGGCATCCACGAAAC-3′ (forward) and 5′-AAGCATTTGCGGTGGACGATGGAG-3′ (reverse).

Western blot analysis

Cells were lysed in NP40 lysis buffer (50 mM Tris [pH 8.0], 137 mM NaCl, 1% NP40, 10% glycerol, 1 mM Na_3VO_4, 1 mM PMSF, protease inhibitor mixture [Sigma-Aldrich]) on ice. Western blotting to detect GlyRα2 in human neutrophils and in human embryonic kidney (HEK)-293 cell line transfected with GlyRα2 was carried out using anti-GlyRα2 Ab (N-18) at a 1:1000 dilution. Blocking peptide was from Santa Cruz Biotechnology. Anti-actin Ab was used as a loading control. For detection of tagged TRPM2 protein in HEK-293–TRPM2 cell line, monoclonal anti-FLAG Ab (Sigma-Aldrich) was used at a 1:5000 dilution. The presence of target proteins was detected by the chemiluminescence method (Amersham Biosciences, Arlington Heights, IL).

Immunofluorescence microscopy

Neutrophils were fixed using 2% paraformaldehyde for 15 min at room temperature. The cells were then permeabilized using 0.05% Triton X-100 for 10 min at room temperature. After 1-h blocking period in PBS containing 3% BSA, the neutrophils were incubated for 1 h with a goat anti-GlyRα2 Ab (N-18) that was used at a 1:25 dilution in blocking buffer. After 1-h incubation at room temperature, cells were washed three times in PBS and were incubated for 1 h with the Alexa Fluor 594 rabbit anti-goat IgG F(ab′)2 used at a final dilution of 1:500. After three washes in PBS, the cells were mounted using mounting medium. Visual inspection and recording of images were performed using a Zeiss LMS 510 laser scanning confocal microscope (Carl Zeiss).

Transfection with microRNA-adapted shRNA of GlyRα2 and TRPM2

The sequences of shRNAmir targeting GlyRα2 and TRPM2 were as follows: shRNAmir against GlyRα2 ; 5′-TGC-TGT-TGA-CAG-TGA-GCG-CCC-AGT-AAA-CGT-TAC-TTG-CAA-TTA-GTG-AAG-CCA-CAG-ATG-TAA-TTG-CAA-GTA-ACG-TTT-ACT-GGA-TGC-CTA-CTG-CCT-CGG-A-3′, shRNAmir against TRPM2; 5′-TGC-TGT-TGA-CAG-TGA-GCG-ACC-TGC-TAT-CCT-GGG-AGA-TCT-ATA-GTG-AAG-CCA-CAG-ATG-TAT-AGA-TCT-CCC-AGG-ATA-GCA-GGG-TGC-CTA-CTG-CCT-CGG-A-3′ (underlined sequences represent mature shRNA). Neutrophils were transfected with short hairpin RNA using the Amaxa Nucleofector Technology. Transfection was performed according to the manufacturer's instructions. In brief, 1×10^7 neutrophils were resuspended in human monocyte nucleofector solution (100 μl) of human monocyte transfector kit (Amaxa Biosystems, Cologne, Germany) at room temperature, followed by addition of 3 μg shRNAmir against Glyα2, shRNA against TRPM2, pmaxGFP, or control shRNAmir. Transfection was performed in an Amaxa Nucleofector II using program Y-001. Immediately afterward, neutrophils were diluted in 2.5 ml human nucleofector medium and incubated for 24 h in a humidified CO_2 incubator. For evaluation of general transfection efficiency, pmaxGFP expression in transfected cells at 24 h was determined by FACS analysis. Neutrophils were harvested and fixed with BD cytofix and pmaxGFP expression was measured in a Guava EasyCyte (Guava Technologies, Hayward, CA).

Fluorescence measurement of MQAE

Measurement of $[Cl^-]_i$ using MQAE fluorescence was performed as described previously (25). Briefly, neutrophils were loaded with 5 mM MQAE in Tyrode solution for 60 min at 37°C. Tyrode solution consisted of (in mM) NaCl 140, KCl 5, $MgCl_2$ 0.25, glucose 5.5, $CaCl_2$ 1.5, HEPES 10, and pH was adjusted to 7.4 with NaOH. After washing with Tyrode so-

lution twice, MQAE-loaded neutrophils were resuspended in Tyrode solution supplemented with 5% FBS and 133 μM glycine, and 4×10^6/ml neutrophils were plated on 96-well plate. MQAE-loaded neutrophils were pretreated with strychnine (1 μM), anti-G2A Ab (1 μg/ml), PTX (2.5 μg/ml), or vehicle (0.1% DMSO v/v) before LPC treatment. For PTX and anti-G2A Ab, neutrophils were pretreated for 1–2 h. Traces of MQAE fluorescence were recorded with Spectramax M2/e fluorescence microplate reader (Molecular Devices) at 360 nm excitation and 460 nm emission. MQAE fluorescence intensity was subtracted with average intensity during 5 min prior to the addition of LPC.

Calibration of $[Cl^-]_i$

Calibration of intracellular MQAE was performed as previously described (26). The relationship between MQAE fluorescence intensity and chloride concentration is calibrated by Stern-Volmer equation. To evaluate maximal fluorescence intensity (F_o), MQAE-loaded neutrophils were incubated in chloride-free medium, and intracellular chloride was depleted by adding nigericin (7 μM) and tributyltin (10 μM). Then, correlation curve between MQAE fluorescence and chloride concentration was obtained by incubating neutrophils in different concentrations of chloride (0, 10, 20, 40, 100, and 140 mM). At the end of each experiment, MQAE fluorescence was quenched by adding KSCN (150 mM) and valinomycin (5 μM). MQAE fluorescence at given chloride concentration was subtracted with F_{KSCN}. In our experimental condition, K_{sv} is 0.082. Average MQAE fluorescence intensity for 15 min after the addition of LPC was obtained for calibration of $[Cl^-]_i$.

Fluorescence measurement of Fluo-3

$[Ca^{2+}]_i$ was measured using the fluorescent Ca^{2+} indicator Fluo-3. Neutrophils were loaded with Fluo-3 AM (4 μM) in HEPES physiologic salt solution (HEPES-PSS) (in mM) (NaCl 140, KCl 5, $MgCl_2$ 1, $CaCl_2$ 1, Glucose 10, HEPES 10) for 30 min at 37°C. After washing with HEPES-PSS, Fluo-3 AM-loaded neutrophils were resuspended in HEPES-PSS supplemented with 5% FBS and 133 μM glycine and plated on 96-well plates at a cell density of 3×10^6/ml. Inhibitors (strychnine 1 μM, econazole 1 μM, clotrimazole 1 μM, or flufenamic acid 1 μM) were pretreated for 15 min before LPC treatment. Traces of intracellular calcium in Fluo-3 AM-loaded neutrophils were measured at 490 nm/526 nm using Spectramax M2/e fluorescence microplate reader (Molecular Devices). Fluorescent emission readings were recorded every 10 s. Raw fluorescence was subtracted with average fluorescence during 5 min before the addition of LPC. In some experiments, Fluo-3 AM-loaded neutrophils were pretreated with E. coli for 20 min and unengulfed E. coli were washed out before LPC treament.

Cell culture

TRPM2-transfected HEK-293 cells were maintained in DMEM supplemented with 10% FBS, and penicillin (100 U/ml) and streptomycin (100 U/ml) at 37°C in a 5% CO_2 incubator. To induce the expression of TRPM2, cells were incubated with doxycycline (1 μg/ml) for at least 24 h prior to experiments.

Intracellular injection of chloride or ADPR

Intracellular injection was performed as described previously (27). TRPM2-transfected HEK-293 cells were cultured on a 35-mm dish before the experiments. Fluo-3 loaded TRPM2-transfected HEK-293 cells were placed on a heated microscope stage. NaCl (150 mM) or Na-gluconate (150 mM) was dissolved in distilled water. ADPR (10 mM) was dissolved in intracellular injection buffer (in mM) (K_2HPO_4 27, Na_2HPO_4 8, KH_2PO_4 26) (pH 7.2). Injection was performed with FemtoJet microinjector, InjectMan NI2 micromanipulator (Eppendorf, Edison, NJ) and finely pulled glass capillaries with a tip inner diameter of 0.5 μm (Femtotip II, Eppendorf). The systems run in the semiautomatic mode with the following instrumental setup conditions: pipette angle 45°, injection pressure 20 hPa, injection time 0.1 s and velocity of the pipette 700 mm/s. Images were acquired using Zeiss LMS 510 laser scanning confocal microscope (Carl Zeiss).

Whole-cell recordings

Glycine-induced anionic currents and TRPM2 current in human peripheral neutrophils and TRPM2 current in HEK-293 cells were studied with the patch clamp technique in the whole-cell mode, using an Axopatch 200B with pClamp 9 and Digidata 1322A (Axon Instruments, Foster City, CA) or EPC-9 amplifier with Pulse 8.5 software (HEKA, Lamprecht, Germany). Patch pipettes were pulled from borosilicate capillaries (PP-83 puller, Narishige, Tokyo, Japan) with resistances of 4–5 MΩ. Series resistances

were within 15–20 MΩ when held at −60 mV. The data were digitized at a sampling rate 3 kHz and filtered at 10 kHz. A reference electrode made from an Ag-AgCl pellet was connected to the bath through an agar bridge made with 3 M KCl. Pipette and external solution with various Cl^- was used as described in the Supplemental Table. ADPR concentration was 10 μM and Ca^{2+} concentration was adjusted to 1 μM (1.8 mM $CaCl_2$ and 1 mM EGTA) through calculation using the MAXCprogram (www.stanford.edu/cpatton/maxc.html). All experiments were performed at room temperature (22 ± 1°C). The recording chamber was superfused with external solution by gravity at ~10 ml/min.

Statistical analysis

All the statistical data were analyzed by Graphpad Prism 4.0 (GraphPad, San Diego, CA). Survival data were analyzed by the log-rank test. All other data were evaluated either by two-tailed Student *t* test or ANOVA. The Bonferroni test was used for post hoc comparison. Value of $p < 0.05$ was considered to indicate statistical significance.
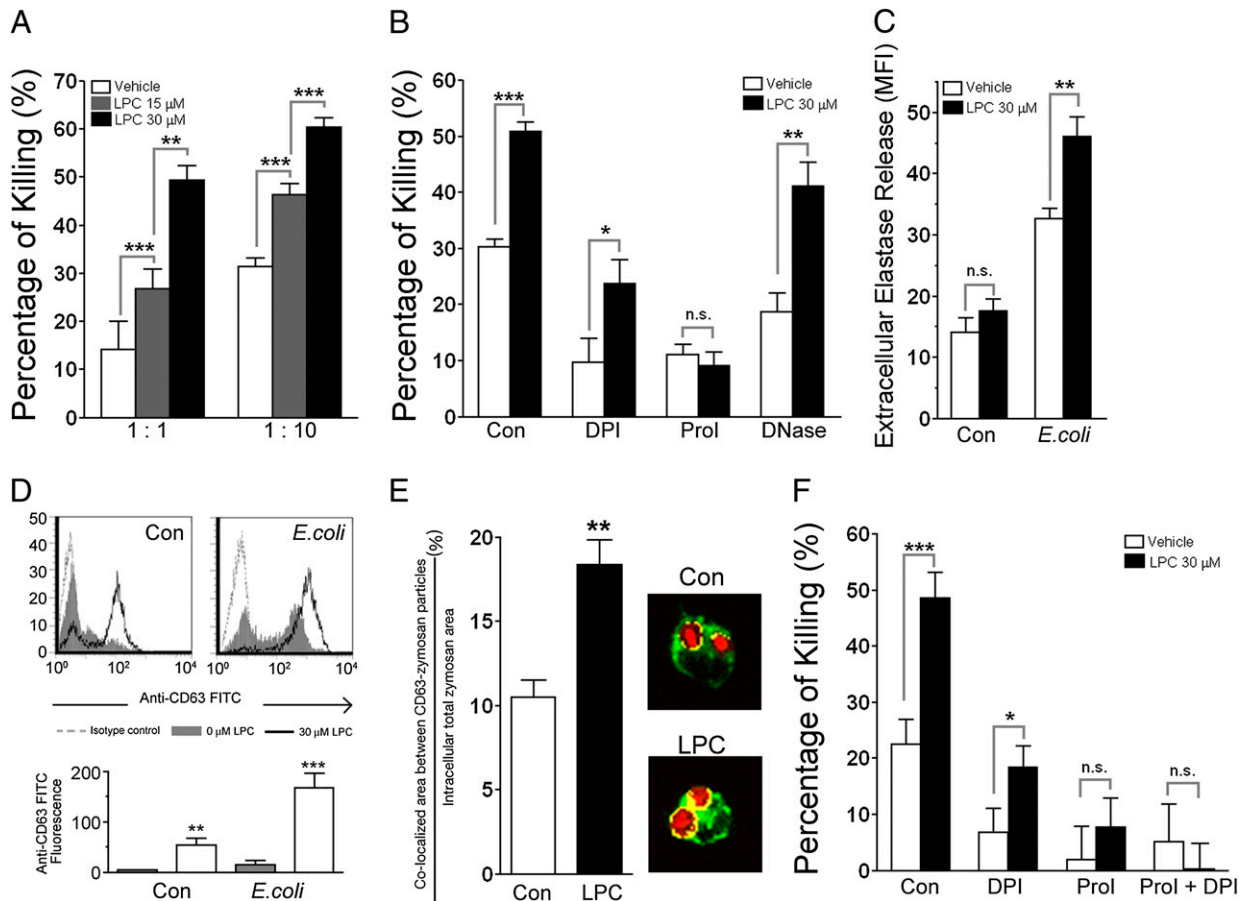
Results

LPC increases E. coli-*killing activity of neutrophils by enhancing azurophil granule-phagosome fusion and elastase release*

As observed with mouse neutrophils (10), LPC effectively enhanced *E. coli*-killing activity in the human neutrophils adhered on a plastic coverslip (Fig. 1*A*): The effective concentrations of

LPC were 15–30 μM in the presence of 5% FBS. Thus, we used a neutrophil/*E. coli* ratio of 1:10, and an LPC concentration of 30 μM in the presence of 5% FBS in subsequent experiments. In a separate assay for bactericidal activity with suspended neutrophils (22, 23), essentially the same result was obtained with LPC (Supplemental Fig. 1).

We first examined the effect of inhibitors of the principal effector systems of neutrophil bactericidal activity (NADPH oxidase, proteases, and neutrophil extracellular traps) by using DPI (28), a mixture of protease inhibitors (17), and DNase (20), respectively. As expected, each of these inhibitors effectively inhibited the basal *E. coli*-killing activity of neutrophils (Fig. 1*B*). Interestingly, however, differential effects of these inhibitors on LPC-enhancement of *E. coli*-killing activity were revealed. The mixture of protease inhibitors totally blocked the LPC effect, DPI (Supplemental Fig. 2) attenuated the LPC effect, whereas DNase did not affect the LPC effect at all (Fig. 1*B*). These results indicate the crucial role of neutrophil proteases in the enhancement by LPC of *E. coli*-killing activity.

Among the neutrophil proteases, elastase plays a critical role in eliminating Gram-negative bacteria, such as *E. coli* (15). Therefore, we examined whether LPC increases the release of elastase.

FIGURE 1. LPC increases *E. coli*-killing activity human neutrophils by enhancing azurophil granule-phagosome fusion and elastase release. *A*, Effects of LPC on bactericidal activity of human neutrophils against *E. coli*. Neutrophils (4×10^6/ml) were exposed to *E. coli* at a ratio of 1:1 and 1:10. *B*, Effects of DPI (1 μM), protease inhibitor mixture (ProI), and DNase (100 U/ml) on LPC-induced enhancement of *E. coli*-killing. *C*, Effects of LPC on extracellular elastase release from neutrophils. Neutrophils were treated with LPC in the presence or absence of *E. coli* for 1 h and then the amount of elastase in the supernatant was measured with Enz Check Elastase assay kit (Molecular Probes). *D*, Surface expression of CD63, a maker of azurophil granules, was measured at 5 min after treatment of LPC to neutrophils that had been allowed to phagocytose *E. coli* for 5 min. Representative FACS histogram (*upper panel*) and bar graphs (*lower panel*) of LPC-induced membrane expression of CD63 in human neutrophils in the presence or absence of *E. coli*. *E*, Bar graph and immunofluorescence microscopy image for effects of LPC on fusion of zymosan-containing phagosome (red) and azurophil granule (CD63; green) in neutrophils are shown. Images were acquired with a ×63 (scan zoom 3) objective. *F*, Effects of DPI (1 μM), and ProI on LPC-induced enhancement of *S. aureus*-killing. *A–F*, An average (± SEM) of more than three experiments is shown. *$p < 0.05$; **$p < 0.01$; ***$p < 0.001$.

Neutrophils were exposed to *E. coli* with or without LPC for 1 h. Exposure to *E. coli* markedly increased the release of elastase, which was significantly enhanced in the presence of LPC (Fig. 1*C*). However, LPC alone (in the absence of *E. coli*) had no significant effect. Elastase is stored in azurophil granules in neutrophils (29). Surface expression of CD63 (Fig. 1*D*), a marker of azurophil granules, measured at 5 min after treatment of LPC to neutrophils that had been allowed to phagocytose *E. coli* for 5 min, showed a similar pattern to the release of elastase (Fig. 1*C*), further indicating the enhanced release of azurophil granules by LPC.

During phagocytosis, even before the phagosome closes, azurophil granule-phagosome fusion begins, and thus the extracellular release of azurophil contents is detected (30–32). Therefore, the LPC-induced enhancement of elastase release from neutrophils exposed to *E. coli* (Fig. 1*C*) suggests an enhanced azurophil granule-phagosome fusion. To confirm this contention, azurophil granule-phagosome fusion was analyzed using human serum-opsonised zymosan, with the same protocol that we used for the bactericidal assay. As shown in Fig. 1*E*, LPC treatment markedly enhanced the colocalization of FITC-labeled CD63 and Alexa 488-labeled zymosan, indicating that LPC markedly enhanced azurophil granule-phagosome fusion.

Next, to test whether the differential effects of a mixture of protease inhibitors and DPI on LPC enhancement of neutrophil bactericidal activity are specific for *E. coli*, we studied *Staph-ylococus aureus*, a Gram-positive bacterium. As shown in Fig. 1*F*, LPC similarly enhanced killing of *S. aureus* by neutrophils. As they did in the presence of *E. coli* (Fig. 1*B*), a mixture of protease inhibitors blocked the LPC effect, and DPI attenuated the LPC effect. These results suggest that the essential role of proteases and the subsidiary role of NADPH oxidase are not limited to Gram-negative bacteria, but extend to Gram-positive bacteria.

LPC-induced enhancement of neutrophil bactericidal activity depends on glycine via GlyR

During literature search for neutrophil bactericidal activity, we came across to a review by Segal, where he suggested an important role for Cl$^-$ flux through GlyRs in neutrophil bactericidal activity, based on unpublished observation (3). The possibility that GlyR is involved in the LPC enhancement of neutrophil bactericidal activity prompted us to examine the effect of strychnine (a GlyR antagonist) on the LPC-induced enhancement of *E. coli*-killing activity. Strikingly, strychnine blocked the LPC effect (Fig. 2*A*), indicating that GlyR critically mediates the LPC activity.

Next, we examined whether strychnine also blocks the LPC-induced enhancement of bacterial clearance in vivo (10). We find that pretreatment of mice with strychnine blocks the LPC-induced enhancement of bacterial clearance in mice with CLP (Fig. 2*B*), and markedly inhibits the protective effect of LPC against CLP-induced lethality (Fig. 2*C*). Strychnine alone did not affect the
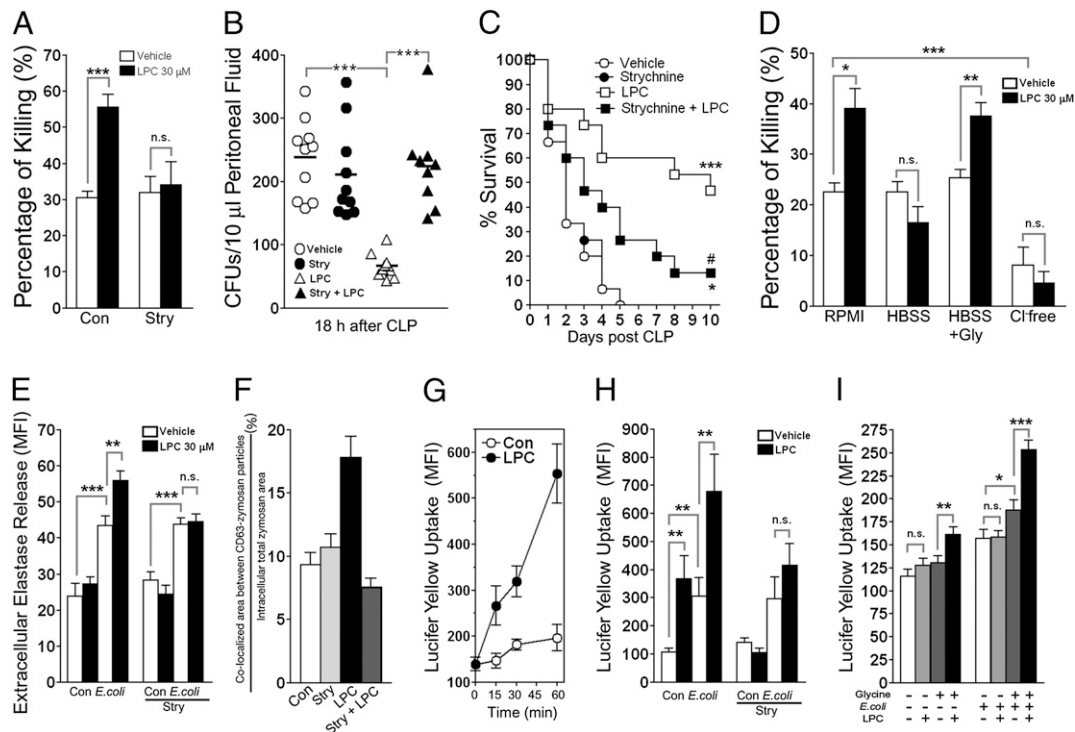
FIGURE 2. LPC-induced enhancement of neutrophil bactericidal activity depends on glycine via GlyR. *A*, Effect of strychnine (1 μM) on LPC-induced enhancement of bactericidal activity. *B*, Clearance of peritoneal bacteria in mice with CLP. Mice were pretreated with PBS or strychnine (0.3 mg/kg, s.c.) 30 min before each injection of vehicle (PBS containing 2% BSA) or LPC (10 mg/kg, s.c.) two times at 2 h and 11 h after CLP. Then, bacterial counts (CFUs) in peritoneal lavage fluid at 18 h after CLP were measured. *n* = 9–10 per group. *C*, Survival was observed in mice after CLP. Mice were pretreated with vehicle (PBS) or strychnine (0.4 mg/kg, s.c.) 30 min before each injection of vehicle (PBS containing 2% BSA) or LPC (10 mg/kg, s.c.) four times at 12 h intervals beginning 2 h after CLP. Log-rank test; *n* = 10 mice per group. *D*, Effects of extracellular glycine and chloride on LPC-induced enhancement of bactericidal activity. HBSS and Gly: HBSS supplemented with 133 μM glycine; Cl$^-$ free: HBSS medium in which chloride was replaced with equimolar amount of gluconate. *E*, Effects of strychnine (1 μM) on LPC-induced enhancement of extracellular release of elastase from neutrophils in the presence or absence of *E. coli*. *F*, Effect of strychnine (1 μM) on fusion of phagosome containing zymosan and azurophil granule (CD63) in neutrophils. *G*, Neutrophils were incubated with 0.5 mg/ml Lucifer yellow for 60 min in the presence or absence of LPC. *H*, Effects of strychnine on LPC-induced enhancement of Lucifer yellow uptake. *I*, Dependence on glycine of LPC-induced enhancement of Lucifer yellow uptake. Note that the *E. coli* in *E*, *H*, and *I* represent neutrophils that were allowed to ingest *E. coli* for 20 min before treatment of LPC. (*A*, *D–I*) An average (± SEM) of more than three experiments is shown. *$p < 0.05$; **$p < 0.01$; ***$p < 0.001$.

basal bacterial clearance, either in vitro (Fig. 2*A*) or in vivo (Fig. 2*B*), nor did it affect CLP-induced lethality in the absence of LPC (Fig. 2*C*).

The RPMI 1640 medium, which we used in our bactericidal assays, contains glycine (133 μM). Thus we asked whether the LPC effect is lost in a medium lacking glycine. In HBSS medium, LPC failed to enhance neutrophil bactericidal activity (Fig. 2*D*). However, when we added glycine to HBSS medium (at a final concentration of 133 μM), the LPC effect was restored (Fig. 2*D*). When chloride was replaced with gluconate in the glycine-supplemented HBSS medium, basal neutrophil bactericidal activity decreased markedly (suggesting the presence of an additional mechanism [apart from GlyR] of chloride modulation of neutrophil bactericidal activity), and the LPC enhancement of bactericidal activity disappeared (Fig. 2*D*). These results clearly show that glycine is essential for LPC enhancement of neutrophil bactericidal activity.

Strychnine blocked the LPC-mediated enhancement of elastase release from neutrophils that were exposed to *E. coli* (Fig. 2*E*). It also blocked the LPC-mediated enhancement of azurophil granule-phagosome fusion (Fig. 2*F*). These results agree with strychnine's blockade of LPC-induced bactericidal activity (Fig. 2*A*). Also, in agreement with its lack of effect on basal bactericidal activity (Fig. 2*A*), strychnine did not affect the basal elastase release from neutrophils exposed to *E. coli* (Fig. 2*E*) and the basal azurophil granule-phagosome fusion (Fig. 2*F*).

Azurophil granule-phagosome fusion with the accompanying release of azurophil granules is a critical step in the bactericidal activity of neutrophils (33, 34). Fittschen and Henson (24) showed that azurophil granule secretion by neutrophils, in response to formyl-methionyl-leucyl-phenylalanine, after cytochalasin B (an inhibitor of actin polymerization) pretreatment is linked to fluid-phase pinocytosis (measured by Lucifer yellow uptake). They

showed that, intriguingly, chloride is essential for both the fluid phase pinocytosis and the accompanying secretion of azurophil granules.

In the current study LPC enhanced the release of elastase, a component of azurophil granules, from *E. coli*-exposed neutrophils. This enhanced release depended on the GlyR, the glycine-operated chloride channel (Fig. 2*E*). These data led us to examine whether LPC enhances fluid-phase pinocytosis, and, if so, whether the enhancement is also dependent on the GlyR. LPC (30 μM) effectively increased Lucifer yellow uptake in resting neutrophils (Fig. 2*G*), and enhanced Lucifer yellow uptake in neutrophils that had ingested *E. coli* (Fig. 2*H*, *left panel*). The enhancement was strychnine-sensitive (Fig. 2*H*). Further in agreement with its lack of effect on basal bactericidal activity (Fig. 2*A*), strychnine did not affect the Lucifer yellow uptake in neutrophils that had phagocytosed *E. coli* in the absence of LPC (Fig. 2*H*, *right panel*). Similar to the essential role of glycine in LPC-induced enhancement of bactericidal activity (Fig. 2*D*), LPC enhancement of Lucifer yellow uptake was also dependent on glycine (Fig. 2*I*). These results indicate that chloride influx via GlyR activated by glycine leads to LPC-induced Lucifer yellow uptake.

The GlyR subtype in human neutrophils is GlyRα2

The existence of GlyR in rat neutrophils was reported (35, 36). However, the existence of GlyR and the identity of its subtype in human neutrophils have not been reported. RT-PCR revealed that GlyRα2 (but not α1, α3, or β) subunit mRNA was present in human neutrophils (Fig. 3*A*). The identity of GlyRα2 subunit mRNA was confirmed by sequencing (data not shown). Western blot analysis revealed GlyRα2 expression in human neutrophils (Fig. 3*B*). These results indicate that human neutrophils contain homomeric GlyRα2. Unexpectedly, confocal GlyRα2 immunofluorescence (using anti-
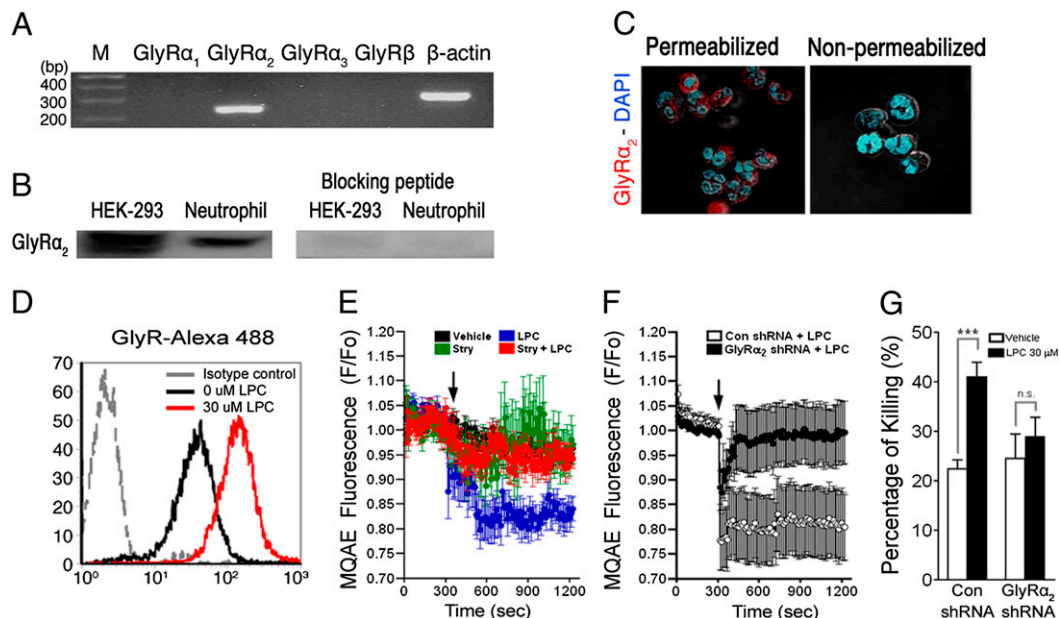
FIGURE 3. LPC induces GlyRα2-mediated $[Cl^-]_i$ increase in neutrophils. *A*, The presence of GlyRα2 in human neutrophils was determined by RT-PCR. *B*, Western blot for GlyRα2 in human neutrophils and GlyRα2-transfected HEK-293 cells as a positive control, with or without blocking peptide against GlyRα2. *C*, Immunofluorescence microscopy of neutrophils stained with anti-GlyRα2 Ab (red). Nuclei were visualized by DAPI stain (blue). Neutrophils were stained with anti-GlyRα2 Ab (red) with or without permeabilization with Triton X-100 (0.05%). Images were acquired with a ×100 (scan zoom 2) objective. *D*, Representative FACS histograms of membrane expression of GlyRα2 in response to LPC. Neutrophils were treated with LPC (30 μM) for 5 min. After fixation, neutrophils were stained with FITC-conjugated anti-GlyRα2 Ab for 30 min. *E* and *F*, Relative intracellular chloride changes in neutrophils were measured with MQAE. Effects of strychnine (*E*) and treatment with shRNA against GlyRα2 (*F*) on LPC-induced decrease in MQAE fluorescence were measured. *G*, Effect of treatment with shRNA against GlyRα2 on LPC-induced enhancement of bactericidal activity was evaluated. An average (± SEM) of more than three experiments is shown. ***$p < 0.001$.

FIGURE 4. Functional expression of glycine-operated channels in human neutrophils. *A* and *B*, representative current-voltage relations (I-V curves) obtained by depolarizing ramp pulses from −100 to 100 mV with KCl pipette solution and normal Tyrode's bath solution before (*A*) and after (*B*) the treatment with 30 μM LPC for 5 min. In the LPC-treated cells, glycine increased the membrane current that crossed the control I-V curve at negative voltage (−50 mV, arrow). *Insets*: Chart traces of membrane currents in response to repetitive ramp pulses from −100 to 100 mV (holding voltage, −60 mV). 0.5 mM glycine was applied in the extracellular solutions as indicated in the Figure. *C*, Summary of outward current amplitudes measured at 60 mV in the above experiments (mean ± SEM, $n = 10$). *$p < 0.05$ compared with preglycine. *D*, Summary of I-V curves (mean ± SEM) in the presence of 0.5 mM glycine obtained in the neutrophils pretreated by LPC (30 μM, $n = 6$) only or with anti-G2A Ab (1 μg/ml, $n = 10$). *$p < 0.05$ compared with anti-G2A Ab-treated cells.
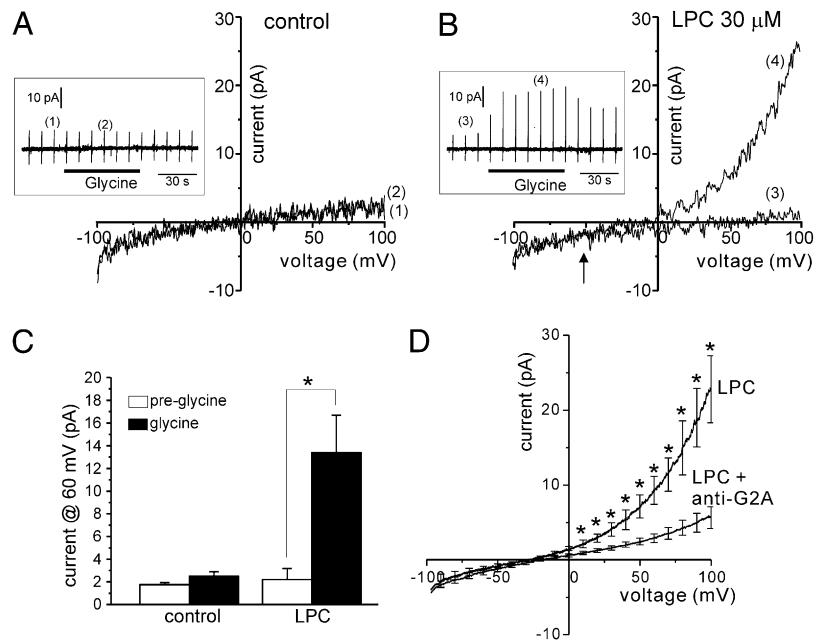
GlyRα2 Ab directed to the extracellular N-terminus of the GlyR) was revealed predominantly in permeabilized neutrophils, indicating that GlyRα2 is mostly located intracellularly in resting neutrophils (Fig. 3*C*). Because extracellular glycine was essential for LPC-induced enhancement of bactericidal activity (Fig. 2*D*) and Lucifer yellow uptake (Fig. 2*I*), we asked whether LPC induces translocation of intracellularly located GlyRα2 to the plasma membrane. As shown in Fig. 3*D*, treatment of neutrophils with LPC for 5 min effectively translocated GlyR to the plasma membrane.

The functional expression of GlyR in human neutrophils was confirmed by whole-cell patch clamp study (Fig. 4). With low-Cl⁻, Cs⁺ pipette solution, an application of glycine (0.5 mM) induced outwardly rectifying current in the LPC (30 μM, 5 min)-pretreated neutorphils, whereas not in the control neutrophils ($n = 8$–10; Fig. 4*A–C*). The current to voltage (I-V) curve with glycine crossed the control I-V curve at negative voltage (∼−60 mV), compatible with the activation of Cl⁻ permeable channels by glycine (Fig. 4*B*,

arrow). To our knowledge, this is the first electrophysiological evidence for the presence of GlyR outside the nervous system.

LPC increases $[Cl^-]_i$ via GlyRα2 in neutrophils

Next, we examined whether LPC increases $[Cl^-]_i$ in neutrophils. $[Cl^-]_i$ was measured using MQAE. The fluorescence of MQAE is decreased by the presence of chloride (37). Fig. 3*E* shows that LPC increases $[Cl^-]_i$, as reflected by the decreased fluorescence of MQAE. Calibration shows that LPC (30 μM) increases $[Cl^-]_i$ of neutrophils from the basal levels of 26.7 ± 2.4 mM (mean ± SEM, $n = 4$) to 35.7 ± 3.3 mM (mean ± SEM, $n = 4$). Because depolarization of membrane potential may lead to subsequent chloride influx, we examined whether LPC depolarizes membrane potential, but found that LPC did not depolarize membrane potential up to 3 min after stimulation, excluding the possibility (Supplemental Fig. 3). The LPC-induced decrease in MQAE fluorescence was blocked by strychnine (Fig. 3*E*), and by treatment with shRNA against GlyRα2 (Fig. 3*F*), indicating that LPC
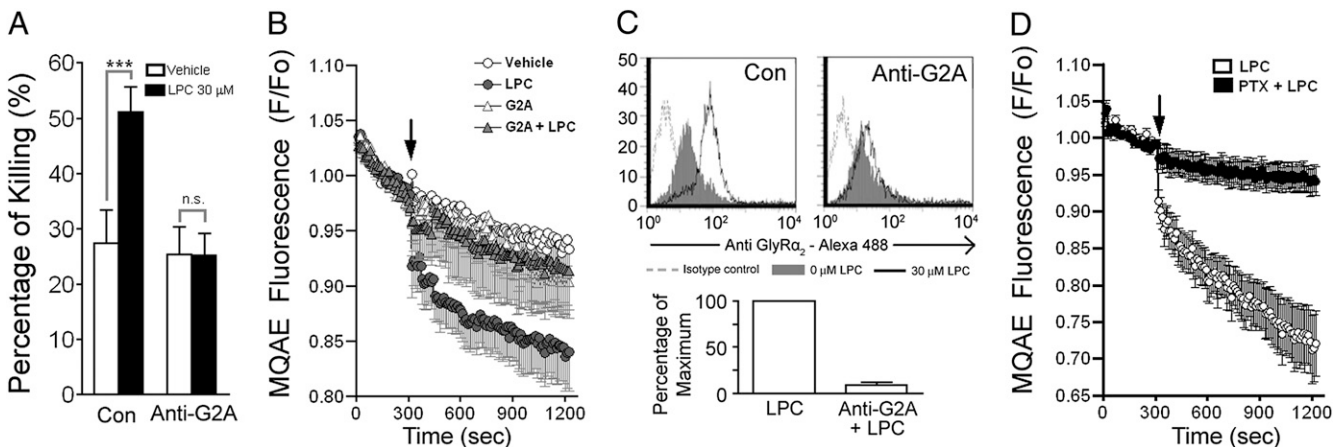
FIGURE 5. LPC increases $[Cl^-]_i$ and GlyR translocation via G2A. *A*, Effect of anti-G2A Ab on LPC-induced enhancement of bactericidal activity. *B*, LPC-induced intracellular chloride changes in neutrophils were measured in the presence of anti-G2A Ab (1 μg/ml). *C*, Representative FACS histogram of membrane expression of GlyRα2 in human neutrophils in response to stimulation of LPC. Neutrphils were pretreated with either anti-G2A Ab (1 μg/ml) or isotype control (normal goat IgG, 1 μg/ml). Bar graph denotes average of more than three independent experiments. *D*, LPC-induced intracellular chloride changes in neutrophils were measured in the presence of PTX (2.5 μg/ml). *B* and *D*, Fluorescence intensity ratio (F/Fo) with the resting fluorescence value Fo in MQAE-loaded neutrophils. LPC was applied at the arrow. *A* and *C*, An average (± SEM) of three experiments is shown. ***$p < 0.001$.

increases $[Cl^-]_i$ via GlyRα2. Furthermore, treatment with shRNA against GlyRα2 abrogated the LPC effect on neutrophil bactericidal activity (Fig. 3*G*). The total amount of GlyRα2 in neutrophils was decreased by 33.9 $\pm$ 8.5% ($p < 0.001$) with shRNA transfection (Supplemental Fig. 4).

LPC induces $[Cl^-]_i$ increase and GlyR translocation via G2A

G2A (for G$_2$ accumulation), a member of G protein-coupled receptor (GPCR) family, has been implicated in lysophopholipid signaling. Many actions of LPC are blocked by anti-G2A Ab (10, 38, 39) or by silencing G2A (40–42) (for review, see Ref. 5). Recently, G2A dimerization/oligomerization resulted from the perturbation of the plasma membrane by insertion of LPC, a conical lipid, was proposed as a mechanism for LPC activation of G2A signaling (39). As observed with mouse neutrophils (10), anti-G2A Ab blocked the LPC-induced enhancement of bactericidal activity in human neutrophils (Fig. 5*A*). Anti-G2A Ab also blocked the LPC-induced $[Cl^-]_i$ increase (Fig. 5*B*) and GlyR translocation (Fig. 5*C*). The conductance increase by LPC in the presence of glycine was also prevented by pretreating neutrophils with anti-G2A Ab (1 μg/ml) (Fig. 4*D*). These results indicate that G2A signaling is upstream to the increase of $[Cl^-]_i$ and GlyR translocation.

Some LPC actions on human neutrophils (9, 39) are blocked by PTX, a Gαi protein blocker. Thus, we examined the effect of PTX

on the LPC-induced $[Cl^-]_i$ increase. The LPC-induced increase of $[Cl^-]_i$ was blocked by PTX (Fig. 5*D*).

LPC induces Ca^{2+} influx via GlyRα_2-mediated $[Cl^-]_i$ increase

$[Ca^{2+}]_i$ in neutrophils is critical for fluid-phase pinocytosis (43), azurophil granule secretion (44, 45) and bactericidal activity (46). Confirming previous reports (9, 39), LPC (30 μM) increased $[Ca^{2+}]_i$ of neutrophils (Fig. 6*A*). In the absence of 5% FBS, LPC (2 μM) induced a similar increase in $[Ca^{2+}]_i$ of neutrophils, suggesting that ~7% of 30 μM LPC in RPMI supplemented with 5% FBS is free (Supplemental Fig. 5). Under conditions where extracellular calcium was removed by calcium-free medium supplemented with 0.3 mM EGTA, LPC could not elevate $[Ca^{2+}]_i$ (Fig. 6*B*), induce Lucifer yellow uptake (Fig. 6*C*), or enhance bactericidal activity (Fig. 6*D*), showing that the LPC-induced enhancement on all these processes is critically dependent on LPC-induced calcium influx.

Because LPC increased both $[Cl^-]_i$ and $[Ca^{2+}]_i$, we hypothesized that LPC-induced $[Cl^-]_i$ increase may lead to $[Ca^{2+}]_i$ increase. Intriguingly, the LPC-induced increase in $[Ca^{2+}]_i$ was markedly inhibited by strychnine (Fig. 6*A*) or treatment with microRNA-adapted shRNA against GlyRα2 (Fig. 6*E*), displaying that $[Cl^-]_i$ increase via GlyRα2 leads to an enhanced calcium influx. Correlating with the requirement of extracellular glycine (133 μM) in LPC-induced enhancement of bactericidal activity (Fig. 2*D*), LPC
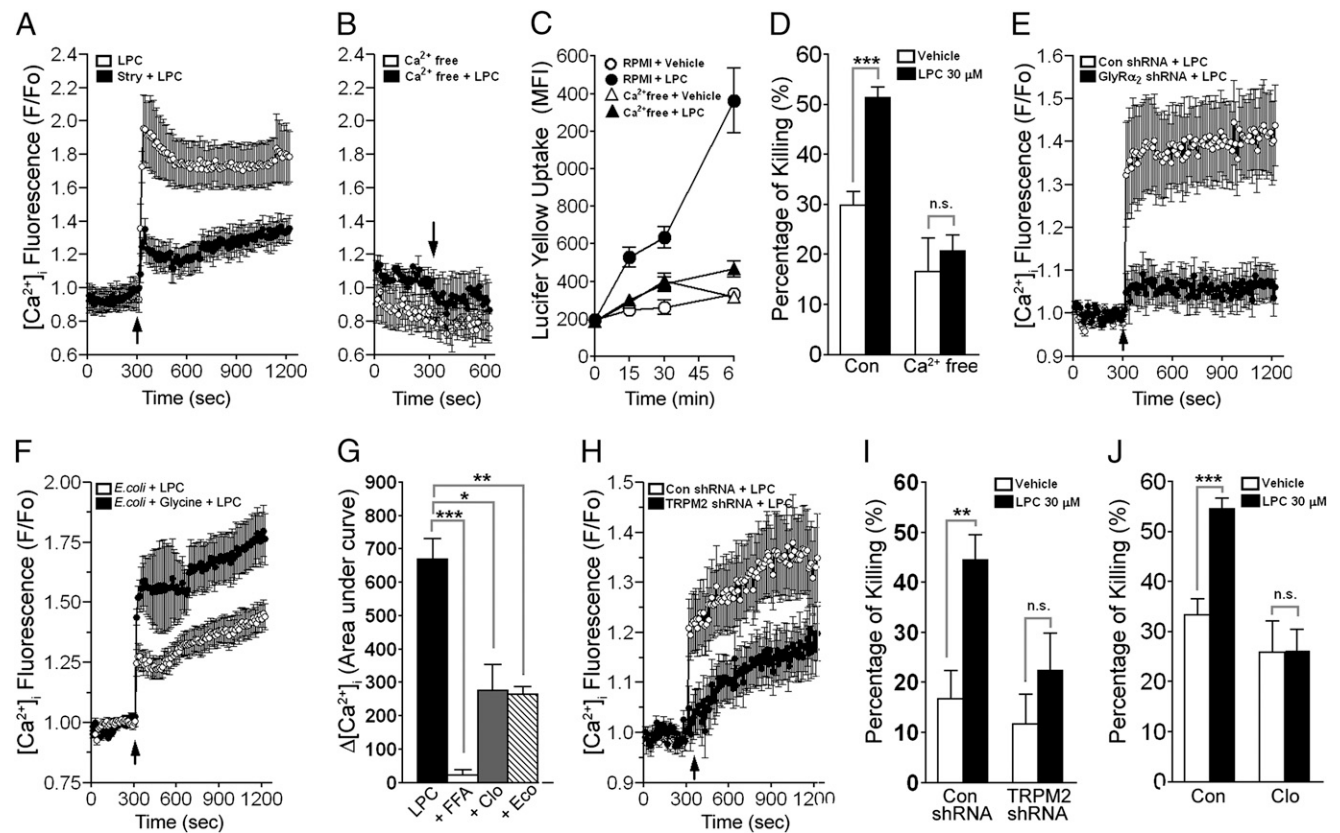
FIGURE 6. LPC induces TRPM2-mediated calcium influx via GlyRα2-mediated $[Cl^-]_i$ increase. *A*, Effect of strychnine (1 μM) on LPC-induced increase in $[Ca^{2+}]_i$. *B–D*, Effects of calcium-free medium (supplemented with 0.3 mM EGTA) on LPC-induced increase in $[Ca^{2+}]_i$ (*B*), Lucifer yellow uptake (*C*), and bactericidal activity (*D*). *E*, Neutrophils were treated with shRNA against GlyRα2 for 24 h, and LPC-induced increase in $[Ca^{2+}]_i$ was measured. *F*, LPC-induced increase in $[Ca^{2+}]_i$ was measured in *E. coli*-ingested neutrophils in the prescence or absence of extracellular glycine (133 μM). *G*, Effects of various inhibitors of TRPM2 on LPC-induced increase in $[Ca^{2+}]_i$. Neutrophils were pretreated with flufenamic acid (100 μM), clotrimazole (25 μM), and econazole (25 μM) for 30 min before the addition of LPC. $\triangle[Ca^{2+}]_i$ represent changes of $[Ca^{2+}]_i$ for 15 min after addition of LPC. *H–J*, Effects of treatment with shRNA against TRPM2 on LPC-induced $[Ca^{2+}]_i$ increase (*H*) and enhancement of bactericidal activity (*I*). Effect of clotrimazole (25 μM) on LPC-induced enhancement of bactericidal activity was also measured (*J*). $[Ca^{2+}]_i$ changes in Fluo-3 AM-loaded neutrophils were expressed as the relative fluorescence intensity over the resting fluorescence value (F/Fo). $\triangle[Ca^{2+}]_i$ is represented as area under curve. LPC was applied at the arrow. *D, G, I and J*, An average ($\pm$ SEM) of three experiments is shown. *$p < 0.05$; **$p < 0.01$; ***$p < 0.001$.

induced a more marked increase in $[Ca^{2+}]_i$ in the presence of glycine in neutrophils that had ingested *E. coli* (Fig. 6*F*).

LPC induces TRPM2-mediated calcium influx

The LPC-induced $[Ca^{2+}]_i$ increase was effectively inhibited by flufenamic acid (100 μM), clotrimazole (25 μM), or econazole (25 μM) (Fig. 6*G*), but not by SKF-96365 (10 μM), ruthenium red (0.2 or 20 μM), Gd^{3+} (50 μM), verapamil (10 μM), or nifedipine (10 μM) (data not shown). This pharmacological profile suggests the involvement of TRPM2, a major TRP channel in neutrophils (47, 48). In neutrophils treated with shRNA against TRPM2 for 24 h, the LPC-induced increases in $[Ca^{2+}]_i$ (Fig. 6*H*) and in neutrophil bactericidal activity (Fig. 6*I*) were markedly inhibited, showing the importance of TRPM2 for the LPC actions. Clotrimazole treatment (25 μM) also blocked LPC-induced enhancement of neutrophil bactericidal activity (Fig. 6*J*).

### Increase in $[Cl^-]_i$ increases TRPM2 channel activity

Next, we hypothesized that the activity of the TRPM2 channel is modulated by $[Cl^-]_i$. Therefore, we asked whether intracellular injection of chloride increases $[Ca^{2+}]_i$ in HEK-293 cells that heterologously express TRPM2. As shown in Fig. 7*A*, intracellular injection of chloride (150 mM NaCl), but not equimolar Na-gluconate, effectively induced an increase of $[Ca^{2+}]_i$ in TRPM2 (+) HEK-293 cells, but not in TRPM2 (−) HEK-293 cells.

ADPR is a major opener of TRPM2 channels (49) and Ca^{2+} is an important positive modulator of TRPM2 (48–51). Therefore, we asked whether ADPR/Ca^{2+}-induced current is sensitive to changes in $[Cl^-]_i$ in TRPM2 (+) HEK-293 cells. $[Cl^-]_i$ was varied from 1 to 100 mM, with $[Cl^-]_e$ being set to equal $[Cl^-]_i$. As shown in Fig. 8*A*, ADPR (10 μM)/Ca^{2+} (1 μM)-induced current was increased as the $[Cl^-]_i$ was increased, indicating that TRPM2 activity is sensitive to $[Cl^-]_i$. The EC_{50} was 17.8 mM, with the peak attained at 50 mM (Fig. 8*B*). It is to be noted that the basal neutrophil $[Cl^-]_i$ (26.7 ± 2.4 mM [mean ± SEM, $n = 4$]) and the LPC-induced $[Cl^-]_i$ (35.7 ± 3.3 mM [mean ± SEM, $n = 4$]) are plotted in the linear region of the curve.

The $[Cl^-]_i$-dependent regulation of TRPM2 activity was also confirmed in neutrophils under the whole-cell clamp conditions. The ionic compositions ($[Cl^-]$) of solution were same with the above experiment of TRPM2 overexpressed in HEK-293 cells. On making the whole-cell configuration with 10 μM ADPR in pipette solution, step-like increase of inward current was observed. The pattern of step-like increase was consistent with the slow kinetics of TRPM2 as described in a previous study of human neutrophils (48). In general, the amplitude of inward was larger with higher $[Cl^-]_i$ (Fig. 8*C*). The inward current was completely reversed by replacing extracellular Na^+ with N-methyl-D-glucamate, a nonpermeable large cation (Fig. 8*D*). No such inward current was observed without ADPR in pipette solution ($n = 10$, data not shown). The amplitudes of inward currents during the initial 80 s after making whole-cell configuration were summarized in a bar graph, which showed $[Cl^-]_i$-dependent facilitation of TRPM2 activation (Fig. 8*E*).

Finally, when TRPM2-transfected HEK cells were rendered to be depleted of intracellular chloride by incubating them for 60–90 min in a medium in which chloride was replaced with gluconate (52), neither H_2O_2, a well-known activating agent for TRPM2 (53,
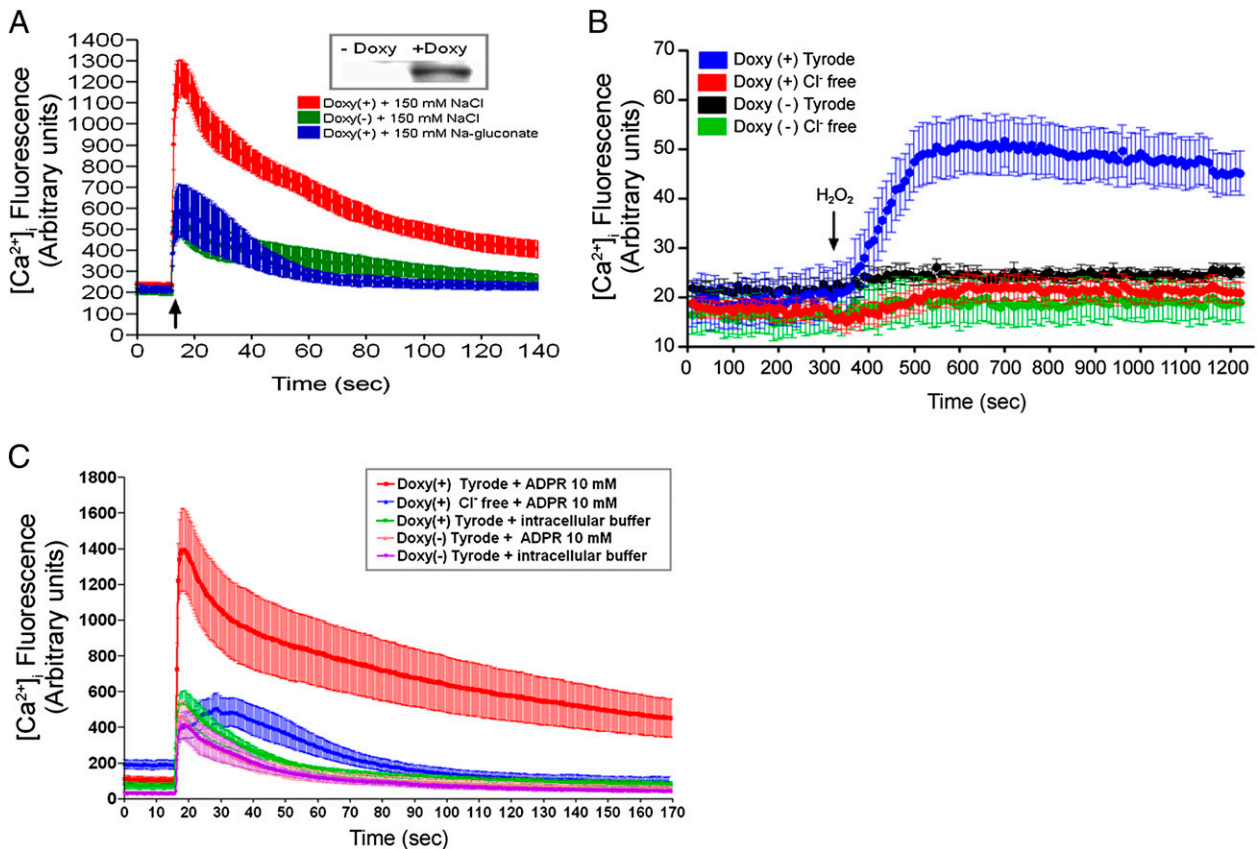
FIGURE 7. TRPM2-mediated $[Ca^{2+}]_i$ increase is sensitive to $[Cl^-]_i$ changes. *A*, Traces of chloride-induced $[Ca^{2+}]_i$ increase in TRPM2-expressing HEK-293 cells. TRPM2-expressing HEK-293 cells were injected with either NaCl or Na-gluconate. Western blot shows doxycyline-responsible TRPM2 expression (*A* inset). *B*, H_2O_2 (1 mM)-induced $[Ca^{2+}]_i$ increase in TRPM2-expressing HEK-293 cells was nearly blocked in chloride-free medium. *C*, Intracellular injection of ADPR (10 mM)-induced $[Ca^{2+}]_i$ increase in TRPM2-expressing HEK-293 cells was nearly blocked in chloride-free medium.
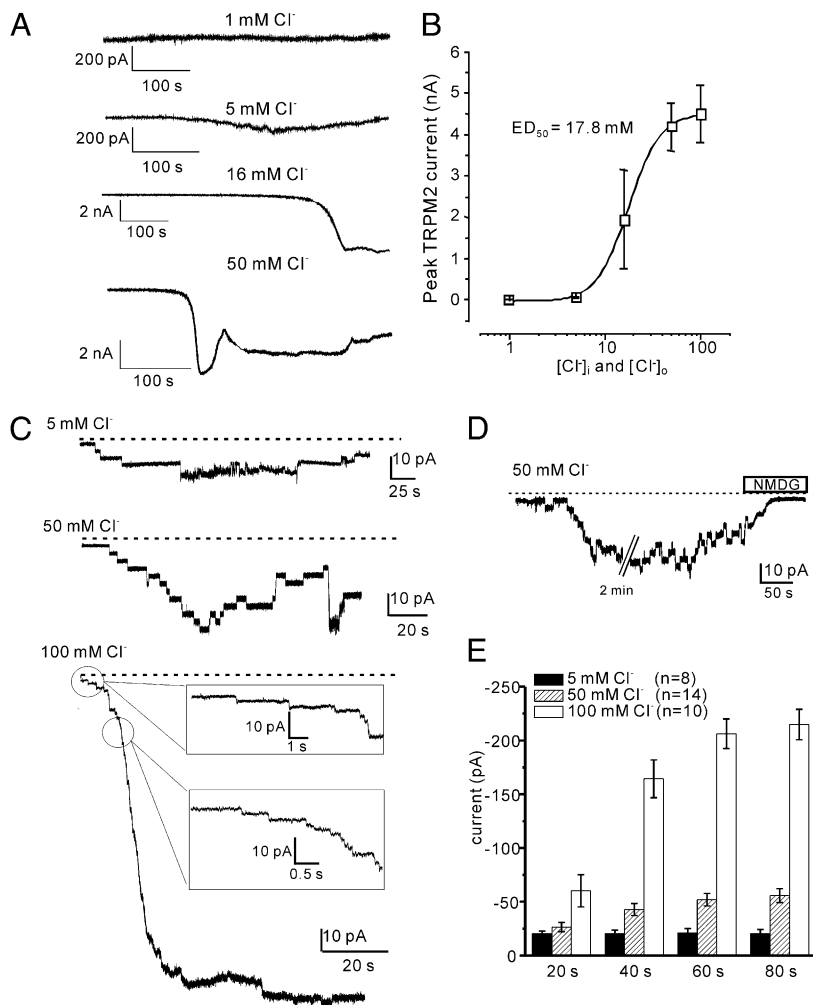
FIGURE 8. Increase in $[Cl^-]_i$ increases TRPM2 channel activity. *A,* ADPR/Ca^{2+}-induced whole-cell currents in TRPM2-expressing HEK-293 cells (holding voltage, -60 mV) with varying concentration of $[Cl^-]_i$. *B,* Peak currents of TRPM2 induced by ADPR/Ca^{2+} in varying concentration of $[Cl^-]$ were averaged and fit with Hill function, to obtain a $[Cl^-]$-dependence of TRPM. The calculated ED_{50} of $[Cl^-]_i$ was 17.8 mM. *C,* Activation of TRPM2 was also confirmed in human neutrophils dialyzed with 10 mM ADPR with different concentrations (5, 50, 100 mM) of Cl^-. Representative current traces after making whole-cell configuration (holding voltage, -60 mV) are shown. Note the step-like increase of inward current in each trace. The characteristic pattern of activation is also shown in the large inward current with 100 mM Cl^- (see *inset* in the *lower panel*). *D,* Abolishment by NMDG of the inward current induced by ADPR with 50 mM Cl^- in neutrophil (holding voltage, -60 mV). *E,* Mean amplitudes of inward currents at 20, 40, 60, and 80 s after making the whole-cell configuration in *C.*

54) (Fig. 7*B*) nor intracellular injection of ADPR (Fig. 7*C*) could elevate $[Ca^{2+}]_i$. These results further show the chloride-sensitive nature of TRPM2.

Involvement of p38 MAPK in LPC actions

p38 MAPK is reported to play a role in azurophil granule release (55, 56). Further, p38 MAPK is involved in phagosomal maturation in macrophage (57). Thus, we asked whether p38 MAPK is involved in LPC-induced enhancement in azurophil granule-phagosome fusion and bactericidal activity. LPC induced p38 phosphorylation, peaking at 5 min after LPC exposure (Fig. 9*A*). The LPC-induced p38 phosphorylation was blocked by strychnine, and in Cl^--free and in Ca^{2+}-free medium (Fig. 9*A*), indicating that GlyR-induced $[Cl^-]_i$-$[Ca^{2+}]_i$ signaling leads to p38 phosphorylation. Further, extracellular glycine was necessary for LPC to induce p38 MAPK phosphorylation (Fig. 9*A*). Together, these results show that both calcium influx and chloride influx are necessary for LPC to induce p38 MAPK phosphporylation.

The p38 MAPK inhibitor SB203580 blocked LPC-induced enhancement in Lucifer yellow uptake (Fig. 9*B*), azurophil granule-phagosome fusion (Fig. 9*C*), and bactericidal activity (Fig. 9*D*). Another p38 MAPK inhibitor SB202190 had essentially the same effects on LPC actions (Supplemental Fig. 6).

Discussion

Thurman and colleagues reported $\alpha2$ and β subunits of GlyR in rat neutrophils (35). However, in human neutrophils, we detected only $\alpha2$ subunit (Fig. 3*A*, 3*B*), indicating that human neutrophils

have homomeric GlyR$\alpha2$. Compared with GlyR$\alpha1\beta$, a major GlyR located synaptically in the adult CNS, homomeric GlyR$\alpha2$ is located nonsynaptically mainly in the fetal brain, has a slower kinetics, and was suggested to function in the paracrine neurotransmitter release (58). This property of homomeric GlyR$\alpha2$ may be well suited for the modulation of neutrophil functions, including granule release.

Thurman and colleagues also reported that glycine inhibits LPS- or fMLP-induced $[Ca^{+2}]_i$ increase in rat neutrophils (36). Their results cannot be directly compared with our results, because of differences in species (rat versus human) with the possible difference in the compositions of GlyR subtypes (35), preparation methods for neutrophils (exudates cells from glycogen-induced peritonitis versus neutrophils purified from venous blood), and stimuli (LPS or fMLP to resting neutrophils versus LPC in the presence of glycine to *E. coli*-ingested neutrophils). It was recently reported that fMLP-induced $[Ca^{+2}]_i$ increase in human neutrophils is potentiated by glycine (59). This finding is more compatible with our results.

The coupling of $[Cl^-]_i$ increase along with $[Ca^{+2}]_i$ increase is a novel signaling mode of neutrophil activation. The core mechanism of the coupling is the sensitivity of TRPM2 activity to $[Cl^-]_i$ (Figs. 7, 8). TRPM2 is gated by ADPR (49) and other various ADPR-related endogenous molecules (for review, see Ref. 60). Furthermore, calcium (48–51) and heat (61) were found to be positive modulators of TRPM2. Our finding that TRPM2 activity is positively modulated by $[Cl^-]_i$ in the presence of ADPR shows a novel mode of chloride action in signal transduction, indicating
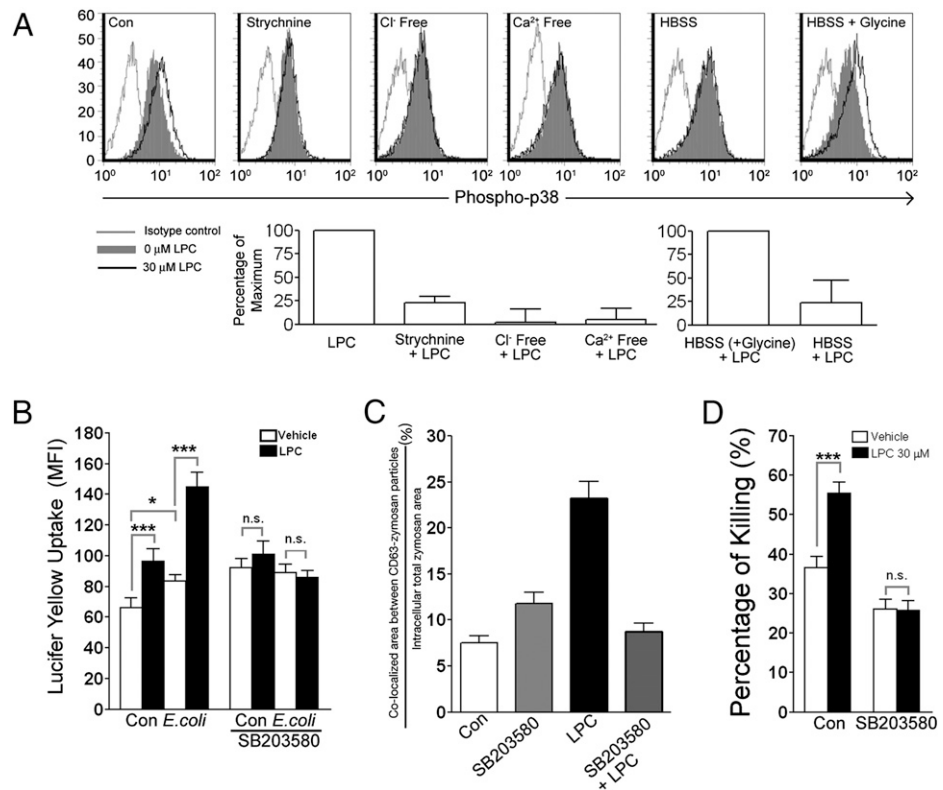
FIGURE 9. LPC induces p38 MAPK phosphorylation, and SB203580 blocks LPC actions. *A*, Representative FACS histogram of LPC-induced p38 MAPK phosphorylation in various conditions. Neutrophils were stimulated with LPC for 5 min, and stained with Alexa 488-conjugated Ab against phospho-p38 after fixation and permeabilization. Isotype controls were shown in gray solid line. Box graphs represent the mean ± SEM of three independent experiments. *B–D*, Effects of SB203580 on LPC-induced enhancement of Lucifer yellow uptake (*B*), azurophil (CD63)-phagosome (zymosan) fusion (*C*), and bactericidal activity (*D*). An average (± SEM) of three experiments is shown. $*p < 0.05$; $***p < 0.001$.

that chloride can be an active player for activating cells equipped with TRPM2. To our knowledge, this is the first evidence for direct modulation by chloride of calcium-conducting channels. Regarding the direct modulation of channels by chloride, it is noteworthy that Cl^--dependent K^+ channels have been reported (62–64).

In multiple cell types, $[Cl^-]_i$ reportedly increases in response to various stimuli (65–68). Furthermore, chloride-sensitive calcium influx, or calcium transients have been reported in several kinds of cells (68–70). However, the exact identity of any chloride-sensitive calcium-conducting channel has not been reported. It would be interesting to examine whether the coupling of increased $[Cl^-]_i$ to TRPM2- (or to other TPR channel(s) which may be sensitive to $[Cl^-]_i$) mediated $[Ca^{+2}]_i$ increase also occurs in these cell types.

TRPM2 is expressed in a wide variety of cells (for review, see Ref. 60). TRPM2 activity is increased by oxidant stress (53, 54), and is involved in oxidant stress-induced cell death (53, 71–73) and chemokine production (74). Therefore, TRPM2 is an important target for the development of therapeutic strategies against oxidative stress-related disorders (for review, see Ref. 60) including inflammation (74). Our finding that $[Cl^-]_i$ is a positive regulator of TRPM2 activity could lead to a novel strategy for modulating this important channel activity.

For LPC enhancement of bactericidal activity against both Gram-positive and Gram-negative bacteria, proteases play a decisive role, whereas the involvement of NADPH oxidase is partial (Fig. 1*B*, 1*F*). Because LPC markedly enhanced the azurophil granule-phagosome fusion, a critical step for killing engulfed micro-organisms (33, 34), it is proposed that LPC enhances neutrophil bactericidal activity ultimately via enhancing the azurophil granule-phagosome fusion with the accompanying proteases release and subsequent protease actions. However, for resting neutrophils, LPC increased Lucifer yellow uptake (Figs. 2*G*, 6*C*), but did not significantly induce elastase release (Fig. 1*C*), suggesting that fluid-phase pinocytosis is permissive but not sufficient for azurophil granule release. LPC-mediated enhancement of elastase

release occurred only with neutrophils that had ingested *E. coli* (Fig. 1*C*). This selectivity could be beneficial, as inappropriately released elastase is potentially destructive to adjacent tissues (75).

Treatment with shRNA against GlyRα2 or strychnine did not affect neutrophil basal bactericidal activity (i.e., activity in the absence of LPC), but did block LPC-mediated enhancement (Figs. 2*A*, 3*G*). Furthermore, treatment with shRNA against TRPM2 (Fig. 6*I*) or clotimazole (Fig. 6*J*) showed a similar pattern. Inhibition of p38 MAPK by SB203580 also did not significantly inhibit basal microbicidal activity, in agreement with previous reports (76, 77), but blocked the LPC effect (Fig. 9*D*). Taken together, these results suggest that the GlyRα2/TRPM2/p38 MAPK signaling is not critically involved in basal bactericidal signaling pathway, but can be mobilized for boosting the bactericidal activity of neutrophils when neutrophils are stimulated by LPC.
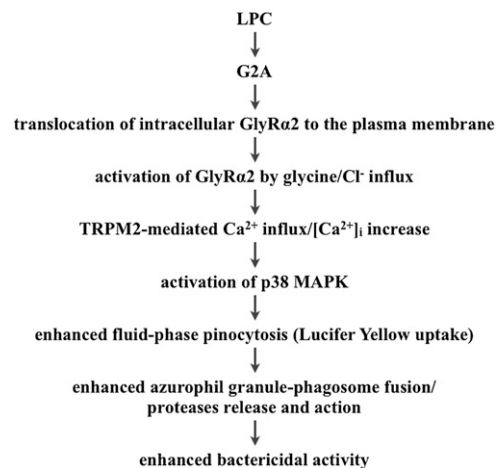
FIGURE 10. Model for LPC-induced enhancement in neutrophil bactericidal activity.

In conclusion, we found the essential role of glycine/GlyRα2, chloride-sensitive TRPM2, and p38 MAPK in the LPC-induced enhancement of bactericidal activity (Fig. 10). Our study proposes that the enhancement of azurophil granule-phagosome fusion via GlyRα2/TRPM2/p38 MAPK signaling is a novel target for enhancing bactericidal activity in neutrophils.

Acknowledgments

Disclosures

References

1. Boucher, H. W., G. H. Talbot, J. S. Bradley, J. E. Edwards, D. Gilbert, L. B. Rice, M. Scheld, B. Spellberg, and J. Bartlett. 2009. Bad bugs, no drugs: no ESKAPE! An update from the Infectious Diseases Society of America. *Clin. Infect. Dis.* 48: 1–12.
2. Spellberg, B., R. Guidos, D. Gilbert, J. Bradley, H. W. Boucher, W. M. Scheld, J. G. Bartlett, and J. Edwards, Jr.; Infectious Diseases Society of America. 2008. The epidemic of antibiotic-resistant infections: a call to action for the medical community from the Infectious Diseases Society of America. *Clin. Infect. Dis.* 46: 155–164.
3. Segal, A. W. 2005. How neutrophils kill microbes. *Annu. Rev. Immunol.* 23: 197–223.
4. Liles, W. C. 2001. Immunomodulatory approaches to augment phagocyte-mediated host defense for treatment of infectious diseases. *Semin. Respir. Infect.* 16: 11–17.
5. Kabarowski, J. H. 2009. G2A and LPC: regulatory functions in immunity. *Prostaglandins Other Lipid Mediat.* 89: 73–81.
6. Englberger, W., D. Bitter-Suermann, and U. Hadding. 1987. Influence of lysophospholipids and PAF on the oxidative burst of PMNL. *Int. J. Immunopharmacol.* 9: 275–282.
7. Lin, P., E. J. Welch, X. P. Gao, A. B. Malik, and R. D. Ye. 2005. Lysophosphatidylcholine modulates neutrophil oxidant production through elevation of cyclic AMP. *J. Immunol.* 174: 2981–2989.
8. Müller, J., M. Petković, J. Schiller, K. Arnold, S. Reichl, and J. Arnhold. 2002. Effects of lysophospholipids on the generation of reactive oxygen species by fMLP- and PMA-stimulated human neutrophils. *Luminescence* 17: 141–149.
9. Silliman, C. C., D. J. Elzi, D. R. Ambruso, R. J. Musters, C. Hamiel, R. J. Harbeck, A. J. Paterson, A. J. Bjornsen, T. H. Wyman, M. Kelher, et al. 2003. Lysophosphatidylcholines prime the NADPH oxidase and stimulate multiple neutrophil functions through changes in cytosolic calcium. *J. Leukoc. Biol.* 73: 511–524.
10. Yan, J. J., J. S. Jung, J. E. Lee, J. Lee, S. O. Huh, H. S. Kim, K. C. Jung, J. Y. Cho, J. S. Nam, H. W. Suh, et al. 2004. Therapeutic effects of lysophosphatidylcholine in experimental sepsis. *Nat. Med.* 10: 161–167.
11. Ginsburg, I., P. A. Ward, and J. Varani. 1989. Lysophosphatides enhance superoxide responses of stimulated human neutrophils. *Inflammation* 13: 163–174.
12. Nishioka, H., H. Horiuchi, H. Arai, and T. Kita. 1998. Lysophosphatidylcholine generates superoxide anions through activation of phosphatidylinositol 3-kinase in human neutrophils. *FEBS Lett.* 441: 63–66.
13. Savage, J. E., A. J. Theron, and R. Anderson. 1993. Activation of neutrophil membrane-associated oxidative metabolism by ultraviolet radiation. *J. Invest. Dermatol.* 101: 532–536.
14. Roos, D., R. van Bruggen, and C. Meischl. 2003. Oxidative killing of microbes by neutrophils. *Microbes Infect.* 5: 1307–1315.
15. Belaaouaj, A., R. McCarthy, M. Baumann, Z. Gao, T. J. Ley, S. N. Abraham, and S. D. Shapiro. 1998. Mice lacking neutrophil elastase reveal impaired host defense against gram negative bacterial sepsis. *Nat. Med.* 4: 615–618.
16. Garcia, R., L. Gusmani, R. Murgia, C. Guarnaccia, M. Cinco, and G. Rottini. 1998. Elastase is the only human neutrophil granule protein that alone is responsible for in vitro killing of *Borrelia burgdorferi*. *Infect. Immun.* 66: 1408–1412.
17. Reeves, E. P., H. Lu, H. L. Jacobs, C. G. Messina, S. Bolsover, G. Gabella, E. O. Potma, A. Warley, J. Roes, and A. W. Segal. 2002. Killing activity of neutrophils is mediated through activation of proteases by K$^+$ flux. *Nature* 416: 291–297.
18. Tkalcevic, J., M. Novelli, M. Phylactides, J. P. Iredale, A. W. Segal, and J. Roes. 2000. Impaired immunity and enhanced resistance to endotoxin in the absence of neutrophil elastase and cathepsin G. *Immunity* 12: 201–210.
19. Nauseef, W. M. 2007. How human neutrophils kill and degrade microbes: an integrated view. *Immunol. Rev.* 219: 88–102.
20. Brinkmann, V., U. Reichard, C. Goosmann, B. Fauler, Y. Uhlemann, D. S. Weiss, Y. Weinrauch, and A. Zychlinsky. 2004. Neutrophil extracellular traps kill bacteria. *Science* 303: 1532–1535.
21. Qureshi, M. A., and R. R. Dietert. 1995. Bacterial uptake and killing by macrophages. In *Methods in Immunotoxicology*. G. R. Burleson, J. H. Dean, and A. E. Munson, eds. Wiley-Liss, New York, p. 119–131.
22. Heo, S. K., S. A. Ju, S. C. Lee, S. M. Park, S. Y. Choe, B. Kwon, B. S. Kwon, and B. S. Kim. 2006. LIGHT enhances the bactericidal activity of human monocytes and neutrophils via HVEM. *J. Leukoc. Biol.* 79: 330–338.
23. Leijh, P. C., M. T. van den Barselaar, T. L. van Zwet, M. R. Daha, and R. van Furth. 1979. Requirement of extracellular complement and immunoglobulin for intracellular killing of micro-organisms by human monocytes. *J. Clin. Invest.* 63: 772–784.
24. Fittschen, C., and P. M. Henson. 1994. Linkage of azurophil granule secretion in neutrophils to chloride ion transport and endosomal transcytosis. *J. Clin. Invest.* 93: 247–255.
25. Lai, Z. F., Y. Z. Chen, and K. Nishi. 2003. Modulation of intracellular Cl⁻-homeostasis by lectin-stimulation in Jurkat T lymphocytes. *Eur. J. Pharmacol.* 482: 1–8.
26. Krapf, R., C. A. Berry, and A. S. Verkman. 1988. Estimation of intracellular chloride activity in isolated perfused rabbit proximal convoluted tubules using a fluorescent indicator. *Biophys. J.* 53: 955–962.
27. Gasser, A., G. Glassmeier, R. Fliegert, M. F. Langhorst, S. Meinke, D. Hein, S. Krüger, K. Weber, I. Heiner, N. Oppenheimer, et al. 2006. Activation of T cell calcium influx by the second messenger ADP-ribose. *J. Biol. Chem.* 281: 2489–2496.
28. Doussière, J., and P. V. Vignais. 1992. Diphenylene iodonium as an inhibitor of the NADPH oxidase complex of bovine neutrophils. Factors controlling the inhibitory potency of diphenylene iodonium in a cell-free system of oxidase activation. *Eur. J. Biochem.* 208: 61–71.
29. Ohlsson, K., and I. Olsson. 1974. The neutral proteases of human granulocytes. Isolation and partial characterization of granulocyte elastases. *Eur. J. Biochem.* 42: 519–527.
30. Pryzwansky, K. B., E. K. MacRae, J. K. Spitznagel, and M. H. Cooney. 1979. Early degranulation of human neutrophils: immunocytochemical studies of surface and intracellular phagocytic events. *Cell* 18: 1025–1033.
31. Segal, A. W., J. Dorling, and S. Coade. 1980. Kinetics of fusion of the cytoplasmic granules with phagocytic vacuoles in human polymorphonuclear leukocytes. Biochemical and morphological studies. *J. Cell Biol.* 85: 42–59.
32. Tapper, H., and S. Grinstein. 1997. Fc receptor-triggered insertion of secretory granules into the plasma membrane of human neutrophils: selective retrieval during phagocytosis. *J. Immunol.* 159: 409–418.
33. Abramson, J. S., J. C. Lewis, D. S. Lyles, K. A. Heller, E. L. Mills, and D. A. Bass. 1982. Inhibition of neutrophil lysosome-phagosome fusion associated with influenza virus infection in vitro. Role in depressed bactericidal activity. *J. Clin. Invest.* 69: 1393–1397.
34. Staali, L., S. Bauer, M. Mörgelin, L. Björck, and H. Tapper. 2006. *Streptococcus pyogenes* bacteria modulate membrane traffic in human neutrophils and selectively inhibit azurophilic granule fusion with phagosomes. *Cell. Microbiol.* 8: 690–703.
35. Froh, M., R. G. Thurman, and M. D. Wheeler. 2002. Molecular evidence for a glycine-gated chloride channel in macrophages and leukocytes. *Am. J. Physiol. Gastrointest. Liver Physiol.* 283: G856–G863.
36. Wheeler, M., R. F. Stachlewitz, S. Yamashina, K. Ikejima, A. L. Morrow, and R. G. Thurman. 2000. Glycine-gated chloride channels in neutrophils attenuate calcium influx and superoxide production. *FASEB J.* 14: 476–484.
37. Verkman, A. S., M. C. Sellers, A. C. Chao, T. Leung, and R. Ketcham. 1989. Synthesis and characterization of improved chloride-sensitive fluorescent indicators for biological applications. *Anal. Biochem.* 178: 355–361.
38. Chen, G., J. Li, X. Qiang, C. J. Czura, M. Ochani, K. Ochani, L. Ulloa, H. Yang, K. J. Tracey, P. Wang, et al. 2005. Suppression of HMGB1 release by stearoyl lysophosphatidylcholine:an additional mechanism for its therapeutic effects in experimental sepsis. *J. Lipid Res.* 46: 623–627.
39. Frasch, S. C., K. Zemski-Berry, R. C. Murphy, N. Borregaard, P. M. Henson, and D. L. Bratton. 2007. Lysophospholipids of different classes mobilize neutrophil secretory vesicles and induce redundant signaling through G2A. *J. Immunol.* 178: 6540–6548.
40. Han, K. H., K. H. Hong, J. Ko, K. S. Rhee, M. K. Hong, J. J. Kim, Y. H. Kim, and S. J. Park. 2004. Lysophosphatidylcholine up-regulates CXCR4 chemokine receptor expression in human CD4 T cells. *J. Leukoc. Biol.* 76: 195–202.
41. Radu, C. G., L. V. Yang, M. Riedinger, M. Au, and O. N. Witte. 2004. T cell chemotaxis to lysophosphatidylcholine through the G2A receptor. *Proc. Natl. Acad. Sci. USA* 101: 245–250.
42. Yang, L. V., C. G. Radu, L. Wang, M. Riedinger, and O. N. Witte. 2005. Gi-independent macrophage chemotaxis to lysophosphatidylcholine via the immunoregulatory GPCR G2A. *Blood* 105: 1127–1134.
43. Botelho, R. J., H. Tapper, W. Furuya, D. Mojdami, and S. Grinstein. 2002. Fc gamma R-mediated phagocytosis stimulates localized pinocytosis in human neutrophils. *J. Immunol.* 169: 4423–4429.
44. Lew, P. D., A. Monod, F. A. Waldvogel, B. Dewald, M. Baggiolini, and T. Pozzan. 1986. Quantitative analysis of the cytosolic free calcium dependency of exocytosis from three subcellular compartments in intact human neutrophils. *J. Cell Biol.* 102: 2197–2204.
45. Tapper, H., W. Furuya, and S. Grinstein. 2002. Localized exocytosis of primary (lysosomal) granules during phagocytosis: role of Ca^{2+}-dependent tyrosine phosphorylation and microtubules. *J. Immunol.* 168: 5287–5296.

46. Wilsson, A., H. Lundqvist, M. Gustafsson, and O. Stendahl. 1996. Killing of phagocytosed *Staphylococcus aureus* by human neutrophils requires intracellular free calcium. *J. Leukoc. Biol.* 59: 902–907.

47. Heiner, I., J. Eisfeld, C. R. Halaszovich, E. Wehage, E. Jüngling, C. Zitt, and A. Lückhoff. 2003. Expression profile of the transient receptor potential (TRP) family in neutrophil granulocytes: evidence for currents through long TRP channel 2 induced by ADP-ribose and NAD. *Biochem. J.* 371: 1045–1053.

48. Heiner, I., J. Eisfeld, M. Warnstedt, N. Radukina, E. Jüngling, and A. Lückhoff. 2006. Endogenous ADP-ribose enables calcium-regulated cation currents through TRPM2 channels in neutrophil granulocytes. *Biochem. J.* 398: 225–232.

49. Perraud, A. L., A. Fleig, C. A. Dunn, L. A. Bagley, P. Launay, C. Schmitz, A. J. Stokes, Q. Zhu, M. J. Bessman, R. Penner, et al. 2001. ADP-ribose gating of the calcium-permeable LTRPC2 channel revealed by Nudix motif homology. *Nature* 411: 595–599.

50. McHugh, D., R. Flemming, S. Z. Xu, A. L. Perraud, and D. J. Beech. 2003. Critical intracellular Ca2+ dependence of transient receptor potential melastatin 2 (TRPM2) cation channel activation. *J. Biol. Chem.* 278: 11002–11006.

51. Starkus, J., A. Beck, A. Fleig, and R. Penner. 2007. Regulation of TRPM2 by extra- and intracellular calcium. *J. Gen. Physiol.* 130: 427–440.

52. Simchowitz, L., and P. De Weer. 1986. Chloride movements in human neutrophils. Diffusion, exchange, and active transport. *J. Gen. Physiol.* 88: 167–194.

53. Hara, Y., M. Wakamori, M. Ishii, E. Maeno, M. Nishida, T. Yoshida, H. Yamada, S. Shimizu, E. Mori, J. Kudoh, et al. 2002. LTRPC2 Ca2+-permeable channel activated by changes in redox status confers susceptibility to cell death. *Mol. Cell* 9: 163–173.

54. Wehage, E., J. Eisfeld, I. Heiner, E. Jüngling, C. Zitt, and A. Lückhoff. 2002. Activation of the cation channel long transient receptor potential channel 2 (LTRPC2) by hydrogen peroxide. A splice variant reveals a mode of activation independent of ADP-ribose. *J. Biol. Chem.* 277: 23150–23156.

55. Mócsai, A., Z. Jakus, T. Vántus, G. Berton, C. A. Lowell, and E. Ligeti. 2000. Kinase pathways in chemoattractant-induced degranulation of neutrophils: the role of p38 mitogen-activated protein kinase activated by Src family kinases. *J. Immunol.* 164: 4321–4331.

56. Partrick, D. A., E. E. Moore, P. J. Offner, D. R. Meldrum, D. Y. Tamura, J. L. Johnson, and C. C. Silliman. 2000. Maximal human neutrophil priming for superoxide production and elastase release requires p38 mitogen-activated protein kinase activation. *Arch. Surg.* 135: 219–225.

57. Blander, J. M., and R. Medzhitov. 2004. Regulation of phagosome maturation by signals from toll-like receptors. *Science* 304: 1014–1018.

58. Mangin, J. M., M. Baloul, L. Prado De Carvalho, B. Rogister, J. M. Rigo, and P. Legendre. 2003. Kinetic properties of the alpha2 homo-oligomeric glycine receptor impairs a proper synaptic functioning. *J. Physiol.* 553: 369–386.

59. Giambelluca, M. S., and O. A. Gende. 2009. Effect of glycine on the release of reactive oxygen species in human neutrophils. *Int. Immunopharmacol.* 9: 32–37.

60. Eisfeld, J., and A. Luckhoff. 2007. Trpm2. *Handb Exp Pharmacol*:237-252.

61. Togashi, K., Y. Hara, T. Tominaga, T. Higashi, Y. Konishi, Y. Mori, and M. Tominaga. 2006. TRPM2 activation by cyclic ADP-ribose at body temperature is involved in insulin secretion. *EMBO J.* 25: 1804–1815.

62. Bhattacharjee, A., W. J. Joiner, M. Wu, Y. Yang, F. J. Sigworth, and L. K. Kaczmarek. 2003. Slick (Slo2.1), a rapidly-gating sodium-activated potassium channel inhibited by ATP. *J. Neurosci.* 23: 11681–11691.

63. Yuan, A., M. Dourado, A. Butler, N. Walton, A. Wei, and L. Salkoff. 2000. SLO-2, a K+ channel with an unusual Cl- dependence. *Nat. Neurosci.* 3: 771–779.

64. Yuan, A., C. M. Santi, A. Wei, Z. W. Wang, K. Pollak, M. Nonet, L. Kaczmarek, C. M. Crowder, and L. Salkoff. 2003. The sodium-activated potassium channel is encoded by a member of the Slo gene family. *Neuron* 37: 765–773.

65. Inglefield, J. R., and R. D. Schwartz-Bloom. 1998. Optical imaging of hippocampal neurons with a chloride-sensitive dye: early effects of in vitro ischemia. *J. Neurochem.* 70: 2500–2509.

66. Jiang, C., S. Agulian, and G. G. Haddad. 1992. Cl- and Na+ homeostasis during anoxia in rat hypoglossal neurons: intracellular and extracellular in vitro studies. *J. Physiol.* 448: 697–708.

67. Lai, Z. F., and K. Nishi. 1998. Intracellular chloride activity increases in guinea pig ventricular muscle during simulated ischemia. *Am. J. Physiol.* 275: H1613–H1619.

68. Tran, Q. K., H. Watanabe, X. X. Zhang, R. Takahashi, and R. Ohno. 1999. Involvement of myosin light-chain kinase in chloride-sensitive Ca^{2+} influx in porcine aortic endothelial cells. *Cardiovasc. Res.* 44: 623–631.

69. Ma, Y. H., H. W. Wei, K. H. Su, H. E. Ives, and R. C. Morris, Jr. 2004. Chloride-dependent calcium transients induced by angiotensin II in vascular smooth muscle cells. *Am. J. Physiol. Cell Physiol.* 286: C112–C118.

70. Ono, K., M. Nakao, and T. Iijima. 1998. Chloride-sensitive nature of the histamine-induced Ca2+ entry in cultured human aortic endothelial cells. *J. Physiol.* 511: 837–849.

71. Fonfria, E., I. C. Marshall, I. Boyfield, S. D. Skaper, J. P. Hughes, D. E. Owen, W. Zhang, B. A. Miller, C. D. Benham, and S. McNulty. 2005. Amyloid beta-peptide(1-42) and hydrogen peroxide-induced toxicity are mediated by TRPM2 in rat primary striatal cultures. *J. Neurochem.* 95: 715–723.

72. Kaneko, S., S. Kawakami, Y. Hara, M. Wakamori, E. Itoh, T. Minami, Y. Takada, T. Kume, H. Katsuki, Y. Mori, and A. Akaike. 2006. A critical role of TRPM2 in neuronal cell death by hydrogen peroxide. *J. Pharmacol. Sci.* 101: 66–76.

73. McNulty, S., and E. Fonfria. 2005. The role of TRPM channels in cell death. *Pflugers Arch.* 451: 235–242.

74. Yamamoto, S., S. Shimizu, S. Kiyonaka, N. Takahashi, T. Wajima, Y. Hara, T. Negoro, T. Hiroi, Y. Kiuchi, T. Okada, et al. 2008. TRPM2-mediated Ca^{2+} influx induces chemokine production in monocytes that aggravates inflammatory neutrophil infiltration. *Nat. Med.* 14: 738–747.

75. Pham, C. T. 2006. Neutrophil serine proteases: specific regulators of inflammation. *Nat. Rev. Immunol.* 6: 541–550.

76. Schnyder, B., P. C. Meunier, and B. D. Car. 1998. Inhibition of kinases impairs neutrophil activation and killing of *Staphylococcus aureus*. *Biochem. J.* 331: 489–495.

77. Zhong, B., K. Jiang, D. L. Gilvary, P. K. Epling-Burnette, C. Ritchey, J. Liu, R. J. Jackson, E. Hong-Geller, and S. Wei. 2003. Human neutrophils utilize a Rac/Cdc42-dependent MAPK pathway to direct intracellular granule mobilization toward ingested microbial pathogens. *Blood* 101: 3240–3248.